Phase Diagram and Fixed-Point Structure of two dimensional $\mathcal{N} = 1$ Wess-Zumino Models

Franziska Synatschke, Holger Gies and Andreas Wipf
Theoretisch-Physikalisches Institut, Friedrich-Schiller-Universität Jena, Max-Wien-Platz 1, D-07743 Jena, Germany

We study the phases and fixed-point structure of two-dimensional supersymmetric Wess-Zumino models with one supercharge. Our work is based on the functional renormalization group formulated in terms of a manifestly off-shell supersymmetric flow equation for the effective action. Within the derivative expansion, we solve the flow of the superpotential also including the anomalous dimension of the superfield. The models exhibit a surprisingly rich fixed-point structure with a discrete number of fixed-point superpotentials. Each fixed-point superpotential is characterized by its number of nodes and by the number of RG relevant directions. In limiting cases, we find periodic superpotentials and potentials which confine the fields to a compact target space. The maximally IR-attractive fixed point has one relevant direction, the tuning of which distinguishes between supersymmetric and broken phases. For the Wess-Zumino model defined near the Gaußian fixed point, we determine the phase diagram and compute the corresponding ground-state masses.

PACS numbers: 05.10.Cc,12.60.Jv,11.30.Qc

I. INTRODUCTION

Supersymmetry has become a well-received guiding principle in the construction of particle-physics models beyond the standard model. Whereas the resulting phenomenology of these models is often worked out by perturbative analysis, the required breaking of supersymmetry may be of nonperturbative origin; it is therefore typically parameterized into the models by a phenomenological reasoning. For a proper understanding of the underlying dynamical mechanisms of symmetry breaking which is often related to collective condensation phenomena, powerful and flexible nonperturbative methods specifically adapted to supersymmetric theories will eventually be needed.

For many nonperturbative problems in field theory, lattice formulations and simulations have proven successful. As supersymmetry intertwines field transformations with spacetime translations, discretizing spacetime often induces a partial loss of supersymmetry. This problem also goes along with the challenge of properly implementing dynamical fermions on the lattice, currently witnessing significant progress [1–4]. As completely new territory is entered in these studies, nonperturbative continuum methods which can preserve supersymmetry manifestly can complement the lattice studies, eventually leading to a coherent picture.

A promising candidate for a nonperturbative method is the functional renormalization group (RG) which has been successfully applied to a wide range of nonperturbative problems such as critical phenomena, fermionic systems, gauge theories and quantum gravity, see [5–10] for reviews. A number of conceptual studies of supersymmetric theories has already been performed with the functional RG. The delicate point here is, of course, the construction and use of a manifestly supersymmetry-preserving regulator. For instance, a supersymmetric regulator for the $4d$ Wess-Zumino model has been presented in [11, 12]. A functional RG formulation of supersymmetric Yang-Mills theory employing the superfield formalism has been given in [13]; for applications, see also [14, 15]. Recently, general theories of a scalar superfield including the Wess-Zumino model have been investigated with a Polchinski-type RG equation in [16], yielding a new approach to supersymmetric nonrenormalization theorems. A Wilsonian effective action for the Wess-Zumino model by perturbatively iterating the functional RG has been constructed in [17].

This work is devoted to the two-dimensional $\mathcal{N} = 1$ Wess-Zumino model with a general superpotential, exploring the model beyond the realm of perturbative expansions around zero coupling. This is the simplest quantum field theoretic and supersymmetric model where the nonperturbative dynamical aspects of supersymmetry breaking can be studied. The present study details and generalizes our results presented in a recent Letter [18], and builds on our earlier work on supersymmetric quantum mechanics, where we have constructed a manifestly supersymmetric functional RG flow for the anharmonic oscillator [19]; see also [20, 21] for RG studies of supersymmetric quantum mechanics.

Inspired by Witten's work on the potential breaking of supersymmetry in the Wess-Zumino model [22], pioneering nonperturbative lattice studies based on Hamiltonian Monte-Carlo methods had early been performed for this model by Ranft and Schiller [23]. More recently Beccaria and coworkers [24, 25] re-investigated the phase diagram and the ground-state energy of the model with similar methods. Golterman and Petcher [26] formulated a lattice action with a partially realized supersymmetry. Another lattice study of the Wess-Zumino model has been performed by Catterall and Karamov [27]. The results of these studies give a first glimpse into the properties of the phase diagram as will be discussed in Sect. VII.

In the present paper, we use the functional RG equation for the superpotential W to study the phase structure of the $\mathcal{N} = 1$ Wess-Zumino model in two dimen-

sions. In Sect. III, we begin with recalling the off-shell and on-shell effective potentials in a one-loop approximation and comment on certain flaws of the approximations. The main part of this work is concerned with extending and applying the manifestly supersymmetric RG techniques developed in [19] in the context of supersymmetric quantum mechanics. The manifestly supersymmetric flow equation for the effective action is constructed in Sect. IV. To first order in a derivative expansion of the effective action, we solve the RG flow equation for the effective superpotential in Sect. V.

In the fixed-point analysis performed in Sect. VI, already a simple polynomial expansion of the superpotential gives access to an infinite number of fixed points with an increasing number of RG relevant directions. Beyond the polynomial expansion, the flow equation for the full superpotential reveals a variety of qualitatively different solutions depending on the initial conditions: we find periodic, sine-Gordon type solutions as well as sigma-model type solutions confining the field values to a finite interval. At next-to-leading order, a nonzero anomalous dimension governs the large-field asymptotics of the fixed-point superpotentials, such that a family of regular fixed-point solutions arises. This family of superpotentials shows oscillating behavior for small fields and a standard asymptotics for large fields, similar to fixed-point potentials for pure bosonic theories in two dimensions [34, 35]. As a particularity of these supersymmetric models, we identify a new scaling relation between the leading critical exponent of the superpotential flow and the anomalous dimension.

Finally, we study the phase diagram of a particular Wess-Zumino model defined near the Gaußian fixed point in terms of a quadratic superpotential perturbation in Sect. VII. Depending on the initial values of the control parameters of the potential, we observe a quantum phase transition from the supersymmetric to the dynamically broken phase. Following the lattice studies [24, 25, 28], we calculate the critical value of the control parameter for the phase transition as a function of the coupling λ at the cutoff Λ, but now for all values of the coupling λ. We also determine the fermionic and bosonic masses in both phases.

II. WESS-ZUMINO MODEL

Two-dimensional Wess-Zumino models with one supersymmetry are particular Yukawa models where the self-interaction of the scalar field determines the Yukawa coupling. In an off-shell formulation they contain a scalar field ϕ, a Majorana spinor field ψ and an auxiliary field F. To maintain supersymmetry in every step of our calculations we combine these fields to one *real superfield*

$$\Phi(x,\theta) = \phi(x) + \bar{\theta}\gamma_*\psi(x) + \frac{1}{2}(\bar{\theta}\gamma_*\theta)F(x). \tag{1}$$

The anticommuting θ parameter in this expansion is a constant Majorana spinor. Supersymmetry transformations are generated by the supercharges

$$\mathcal{Q} = -i\frac{\partial}{\partial\bar{\theta}} - \partial\!\!\!/\theta, \quad \bar{\mathcal{Q}} = -i\frac{\partial}{\partial\theta} - \bar{\theta}\partial\!\!\!/, \tag{2}$$

which anticommute on space-time translations, $\{\mathcal{Q}_\alpha, \bar{\mathcal{Q}}_\beta\} = 2i\partial\!\!\!/_{\alpha\beta}$. The transformation rules for the component fields are obtained by comparing coefficients in $\delta\Phi = i\bar{\epsilon}[\mathcal{Q}, \Phi]$ and read

$$\begin{aligned} \delta\phi &= \bar{\epsilon}\gamma_*\psi, \quad \delta\psi = (F + i\gamma_*\partial\!\!\!/\phi)\epsilon, \\ \delta\bar{\psi} &= \bar{\epsilon}(F - i\partial\!\!\!/\phi\gamma_*), \quad \delta F = i\bar{\epsilon}\partial\!\!\!/\psi. \end{aligned} \tag{3}$$

As usual the F term transforms into a total derivative such that its space-time integral is invariant under supersymmetry transformations. The supercharges anticommute with the superderivatives

$$\mathcal{D} = \frac{\partial}{\partial\bar{\theta}} + i\partial\!\!\!/\theta, \quad \bar{\mathcal{D}} = -\frac{\partial}{\partial\theta} - i\bar{\theta}\partial\!\!\!/, \tag{4}$$

and up to a sign they obey the same anticommutation rules as the supercharges, $\{\mathcal{D}_\alpha, \bar{\mathcal{D}}_\beta\} = -2i\partial\!\!\!/_{\alpha\beta}$. In explicit calculations, one uses Fierz identities which all follow from

$$\psi\bar{\chi} = -\tfrac{1}{2}\bar{\chi}\psi - \tfrac{1}{2}\gamma_\mu(\bar{\chi}\gamma_\mu\psi) - \tfrac{1}{2}\gamma_*(\bar{\chi}\gamma_*\psi), \tag{5}$$

where $\gamma_* = i\gamma_0\gamma_1$ anti-commutes with the γ_μ. It is useful to keep in mind that for Majorana spinors the fermionic bilinears have the symmetry properties

$$\bar{\psi}\chi = -\bar{\chi}\psi, \ \bar{\psi}\gamma_\mu\chi = -\bar{\chi}\gamma_\mu\psi \quad \text{and} \quad \bar{\psi}\gamma_*\chi = \bar{\chi}\gamma_*\psi, \tag{6}$$

such that the only Lorentz-invariant bilinear is $\bar{\psi}\gamma_*\psi$ since $\bar{\psi}\psi = 0$. Thus, we choose as Lagrangian density $\mathcal{L}_0$ for the free theory the D term of

$$\tfrac{1}{2}\bar{\mathcal{D}}\Phi\gamma_*\mathcal{D}\Phi = \tfrac{1}{2}\bar{\psi}\gamma_*\psi + (\bar{\theta}\gamma_*\psi)F - i\bar{\theta}\gamma^\mu\psi\partial_\mu\phi - \bar{\theta}\gamma_*\theta\mathcal{L}_0. \tag{7}$$

In components it has the form

$$\mathcal{L}_0 = \tfrac{1}{2}\partial_\mu\phi\partial^\mu\phi + \tfrac{i}{4}\bar{\psi}\partial\!\!\!/\psi - \tfrac{i}{4}\partial_\mu\bar{\psi}\gamma^\mu\psi - \tfrac{1}{2}F^2. \tag{8}$$

In this work, we study a class of interacting theories, where the interaction Lagrangian is given by the D term of a superpotential $W(\Phi)$,

$$W(\Phi) = W(\phi) + \bar{\theta}\gamma_*\psi W'(\phi) - \tfrac{1}{2}\bar{\theta}\gamma_*\theta\mathcal{L}_1. \tag{9}$$

In components, $\mathcal{L}_1$ has the form

$$\mathcal{L}_1 = \tfrac{1}{2}W''(\phi)\bar{\psi}\gamma_*\psi - W'(\phi)F. \tag{10}$$

The sum of $\mathcal{L}_0$ and $\mathcal{L}_1$ defines the *off-shell Lagrangian density*

$$\mathcal{L} = \tfrac{1}{2}\partial_\mu\phi\partial^\mu\phi + \tfrac{i}{2}\bar{\psi}\partial\!\!\!/\psi - \tfrac{1}{2}F^2 + \tfrac{1}{2}W''(\phi)\bar{\psi}\gamma_*\psi - W'(\phi)F, \tag{11}$$

which gives rise to an invariant action. As expected for a Euclidean model, this action is unbounded from below and above. After eliminating the auxiliary field via its algebraic equation of motion

$$F = -W'(\phi), \tag{12}$$

we end up with the stable *on-shell Lagrangian density*

$$\mathcal{L} = \tfrac{1}{2}(\partial\phi)^2 + \tfrac{i}{2}\bar\psi\partial\!\!\!/\psi + \tfrac{1}{2}W'^{\,2}(\phi) + \tfrac{1}{2}W''(\phi)\,\bar\psi\gamma_*\psi. \tag{13}$$

This density is invariant under the non-linear on-shell supersymmetry transformations

$$\begin{aligned} \delta\phi = \bar\epsilon\gamma_*\psi, \quad \delta\psi &= \big(i\gamma_*\partial\!\!\!/\phi - W'(\phi)\big)\epsilon, \\ \delta\bar\psi &= \bar\epsilon\big(i\gamma_*\partial\!\!\!/\phi - W'(\phi)\big). \end{aligned} \tag{14}$$

For a polynomial superpotential W the supersymmetric Yukawa models defined in Eq. (11) and (13) are perturbatively super-renormalizable. If the leading term in the superpotential contains an even power of ϕ, $W = c\phi^{2n} + \mathcal{O}(\phi^{2n-1})$, supersymmetry cannot be broken by quantum corrections. However, if the leading term contains an odd power, supersymmetry may be broken.

III. ONE-LOOP PERTURBATION THEORY

Let us first discuss the effective potential in one-loop approximation, which can be set up in both the on-shell or the off-shell formulation. It is well-known that the one-loop on-shell potential becomes artificially complex for non-convex classical potentials [29]. This problem is avoided in the off-shell one-loop formulation: here, keeping first the auxiliary field in the one-loop calculation and subsequently eliminating it by its quantum equation of motion corresponds to a resummation of higher-order terms in the on-shell formulation. We expect that this potential is a better approximation to the exact effective potential as compared to the one-loop on-shell potential. Indeed, we find a real and stable effective potential based on the off-shell calculation. Similar observations can be found in [30]. The corresponding problem in one-dimensional supersymmetric systems has been carefully analyzed by Bergner (see [31] and references therein).

A. On-shell effective potential

To calculate the one-loop potential in the on-shell formulation, we need the fluctuation operators $M_{\rm F}$ and $M_{\rm B}$ for the fermion and the remaining scalar, respectively. For a homogeneous background field ϕ playing the role of a mean field, these operators read

$$\begin{aligned} M_{\rm B} = p^2 + V'' \quad &\text{and} \quad M_{\rm F} = i\partial\!\!\!/ + \gamma_* W'' \\ &\Rightarrow M_{\rm F}^2 = (p^2 + W''^2)\mathbb{1}_2, \end{aligned} \tag{15}$$

where $V = \frac{1}{2}W'^{\,2}$ is the classical potential for the scalar field. In a finite box of size L, the momentum takes the values $p_\mu = 2\pi n_\mu/L$ with integer-valued n_μ. The fermionic integration yields the Pfaffian of $M_{\rm F}$,

$$\mathrm{Pf}(M_{\rm F}) = \pm\sqrt{\det(M_{\rm F})}. \tag{16}$$

We shall assume that the Pfaffian has a fixed sign, such that we may replace the Pfaffian by the square root of the determinant. In a perturbative approach and in the broken phase (with vanishing Witten index), this assumption is justified.

For an operator M with eigenvalues p^2+C^2 the derivative of the zeta function $\zeta_M(s) = \mathrm{tr}(M/\mu^2)^{-s}$ at the origin is

$$\zeta'_M(0) = \frac{(CL)^2}{4\pi}\left(\ln\left(\frac{C}{\mu}\right)^2 - 1 + 4\sum_{n_\mu\neq 0}\frac{K_1(CLn)}{CLn}\right) \tag{17}$$

with the last sum, which involves the MacDonald function, approaching zero exponentially fast with increasing box sizes. Thus, in the thermodynamic limit the one-loop effective potential in the zeta-function scheme is

$$\begin{aligned} U^{(1)}_{\rm on} =& \frac{1}{2}W'^2 + \frac{1}{2L^2}\left(\zeta'_{M_{\rm F}}(0) - \zeta'_{M_{\rm B}}(0)\right) \\ =& \frac{1}{2}W'^2 - \frac{W''^2}{8\pi}[(1+X)\ln(1+X) \\ &+ X\ln(W''/\mu)^2 - X], \end{aligned} \tag{18}$$

with $X = W'W'''/W''^2$. The energy scale μ is fixed by a renormalization condition. If we use a momentum cutoff regularization instead of the ζ-function regularization then we obtain the same result with μ replaced by the cutoff Λ.

The effective potential becomes complex for non-convex classical potentials $V = \frac{1}{2}W'^{\,2}$. To be specific, let us choose

$$W' = \bar\lambda(\phi^2 - \bar a^2) \quad \Rightarrow \quad V = \frac{\bar\lambda^2}{2}(\phi^2 - \bar a^2)^2. \tag{19}$$

For negative $\bar a^2$, the one-loop effective potential is real. For positive $\bar a^2$, it becomes complex for small fields $\phi^2 < \bar a^2/3$. For fields slightly bigger than $\bar a/\sqrt{3}$, the potential is real and *negative*. This signals the failure of the approximation since the effective potential must be non-negative in a supersymmetric theory. Depending on the sign of the renormalized a^2, we find both a supersymmetric phase characterized by a non-vanishing expectation value $\langle\phi\rangle = \phi_{\rm min}$ and $U^{(1)}_{\rm on}(\phi_{\rm min}) = 0$ and a phase with $\langle\phi\rangle = 0$ and broken supersymmetry, see Fig. 1. Here, the renormalization conditions are chosen such that the minimum $\phi_{\rm min}$ agrees with the renormalized value a in the supersymmetric phase. In the broken phase, we use a simple renormalization condition by fixing all parameters at the cutoff, $\mu = \Lambda$. In both cases, the renormalization condition could alternatively be formulated in terms of Coleman-Weinberg renormalization conditions by fixing the curvature of the potential at the minimum to the physical mass.

B. Off-shell effective potential

In the off-shell formulation, the fluctuations of both scalars (including the auxiliary field) and the fermion are taken into account. The off-shell Lagrangian (11) gives rise to the fluctuation operators in the background of both a ϕ and an F mean field,

$$M_{\rm B} = \begin{pmatrix} p^2 - FW''' & -W'' \\ -W'' & -1 \end{pmatrix} \quad \text{and} \quad M_{\rm F} = \not{p} + \gamma_* W'', \tag{20}$$

where the mean fields ϕ (as the argument of W'' and W''') and F are assumed to be homogeneous. It follows that the ζ-function regularized one-loop off-shell potential reads

$$U^{(1)}_{\rm off} = -\frac{1}{2}F^2 - FW' - \frac{W''^2}{8\pi}[(1+Y)\ln(1+Y) + Y\ln(W''/\mu)^2 - Y] \tag{21}$$

with $Y = -FW'''/W''^2$. With a momentum cutoff regularization, we obtain the same result with μ denoting the cutoff. To eliminate the auxiliary field F, we must solve the transcendental gap equation

$$\partial_F U^{(1)}_{\rm off} = -F - W' + \frac{W'''}{8\pi}\ln\frac{(W''^2 - FW''')}{\mu^2} = 0, \tag{22}$$

and insert the solution for F back into $U^{(1)}_{\rm off}$. For an arbitrary ϕ, the gap equation always has a real solution F leading to a real effective potential [32]. Concerning supersymmetry breaking, we find the same qualitative result as with the on-shell calculation: the sign of the renormalized a^2 determines the phase of the system.

Note that the on-shell and off-shell potentials (18) and (21) have similar forms. In Fig. 1 the two potentials are compared with each other and also with the classical potential V. Of course, the same renormalization conditions are used for the on- and off-shell potentials. For positive a^2, the scale parameter μ has been adjusted such that the potentials take their minima at the same value $\phi_{\rm min} = a$. Note that the off-shell potential contains resummed contributions from higher order in $\hbar$. The reason is that the solution F of (22) contains terms of higher order in $\hbar$ and inserting the solution back into the effective potential generates terms to all orders of $\hbar$ in the effective potential. By expanding the off-shell action in $\hbar$, the first-order result agrees again with the complex on-shell effective potential. The effective resummation contained in the off-shell action is such that the effective potential becomes real and non-negative everywhere, in particular, at those points where the classical potential is not convex. For $a^2 > 0$, both one-loop potentials predict a phase with broken $\mathbb{Z}_2$ symmetry and unbroken supersymmetry. For $a^2 < 0$, we find a phase with unbroken $\mathbb{Z}_2$ symmetry and broken supersymmetry.

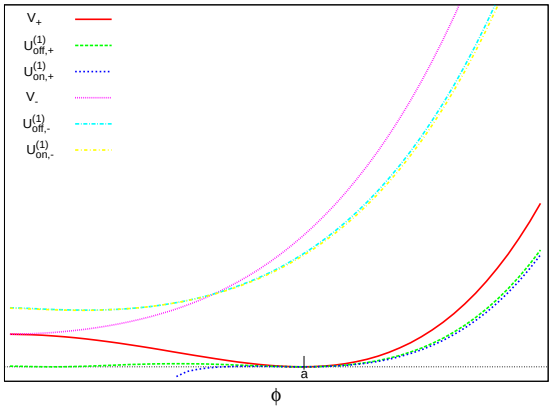

FIG. 1: The classical potential V and the on-shell and off-shell effective potentials $U^{(1)}_{\rm on}$ and $U^{(1)}_{\rm off}$ in one-loop approximation. The subscripts $+$ and $-$ denote the sign of $\bar{a}^2$.

IV. SUPERSYMMETRIC RG FLOW

In this section, we will construct a manifestly supersymmetric flow equation in the off-shell formulation. Our approach is based on the functional RG formulated in terms of a flow equation for the effective average action Γ_k, i.e., the Wetterich equation, [33]

$$\partial_k \Gamma_k = \frac{1}{2}\,{\rm STr}\left\{\left[\Gamma^{(2)}_k + R_k\right]^{-1}\partial_k R_k\right\}. \tag{23}$$

Here, Γ_k is a scale-dependent effective action; it interpolates between the microscopic or classical action S for $k \to \Lambda$, with Λ being the microscopic UV scale, and the full quantum effective action $\Gamma = \Gamma_{k\to 0}$, being the standard generating functional for 1PI correlation functions. The interpolating scale k denotes an infrared IR regulator scale below which all fluctuations with momenta smaller than k are suppressed. For $k \to 0$, all fluctuations are taken into account and we arrive at the full solution of the quantum theory in terms of the effective action Γ. The Wetterich equation defines an RG trajectory in the space of action functionals with the classical action S serving as initial condition.

In Eq. (23), we encounter the second functional derivative of Γ_k,

$$\left(\Gamma^{(2)}_k\right)_{ab} = \frac{\overrightarrow{\delta}}{\delta\Psi_a}\Gamma_k\frac{\overleftarrow{\delta}}{\delta\Psi_b}, \tag{24}$$

where the indices a, b summarize field components, internal and Lorentz indices, as well as spacetime or momentum coordinates. In the present case, we have $\Psi^{\rm T} = (\phi, F, \psi, \bar{\psi})$ where Ψ is not a superfield, but merely a collection of fields. The momentum-dependent regulator function R_k in Eq. (23) establishes the IR suppression of modes below k. In the general case, three properties of the regulator $R_k(p)$ are essential: (i) $R_k(p)|_{p^2/k^2\to 0} > 0$ which implements the IR regularization, (ii) $R_k(p)|_{k^2/p^2\to 0} = 0$ which guarantees that the

regulator vanishes for $k \to 0$, (iii) $R_k(p)|_{k\to\Lambda\to\infty} \to \infty$ which serves to fix the theory at the classical action in the UV. Different functional forms of R_k correspond to different RG trajectories manifesting the RG scheme dependence, but the end point $\Gamma_{k\to 0} \to \Gamma$ remains invariant.

The regularization preserves supersymmetry if the regulator contribution to the action ΔS_K is supersymmetric, see below. As the regulator needs to be quadratic in the fields in order to maintain the one-loop structure of the flow, a general supersymmetric quadratic form can be constructed as a D term of a superfield operator $\Phi K \Phi$. Here, K is a function of the two invariant and commuting operators $\bar{\mathcal{D}}\gamma_*\mathcal{D}$ and $\bar{\mathcal{D}}\not{\partial}\mathcal{D} \propto (\bar{\mathcal{D}}\gamma_*\mathcal{D})^2$. Since powers of $\bar{\mathcal{D}}\gamma_*\mathcal{D}$ boil down to

$$\begin{aligned}(\tfrac{1}{2}\bar{\mathcal{D}}\gamma_*\mathcal{D})^{2n} &= \tfrac{i}{2}\bar{\mathcal{D}}\not{\partial}\mathcal{D}(\partial^2)^{n-1} \quad \text{and} \\ (\tfrac{1}{2}\bar{\mathcal{D}}\gamma_*\mathcal{D})^{2n+1} &= \tfrac{1}{2}\bar{\mathcal{D}}\gamma_*\mathcal{D}(\partial^2)^{n},\end{aligned} \tag{25}$$

where ∂^2 is the standard Laplacian, any invariant and quadratic regulator action is the superspace integral of

$$\frac{1}{2}\Phi\bar{\mathcal{D}}\big(\tilde{r}_1(-\partial^2) - \gamma_* r_2(-\partial^2)\big)\mathcal{D}\Phi. \tag{26}$$

Expressed in component fields, we find

$$\Delta S_k = \frac{1}{2}\int (\phi, F) R_k^{\mathrm{B}} \begin{pmatrix}\phi \\ F\end{pmatrix} + \frac{1}{2}\int \bar{\psi} R_k^{\mathrm{F}} \psi. \tag{27}$$

In momentum space, $i\partial_\mu$ is replaced by p_μ and the operators take the explicit form

$$R_k^{\mathrm{B}} = \begin{pmatrix} p^2 r_2 & -r_1 \\ -r_1 & -r_2\end{pmatrix} \quad \text{and} \quad R_k^{\mathrm{F}} = \not{p}\, r_2 + \gamma_* r_1, \tag{28}$$

where $r_1 = p^2\tilde{r}_1$. Comparison with Eq. (20) reveals that r_1 plays the role of a momentum-dependent supersymmetric mass term, whereas r_2 can be viewed as a deformation of the momentum dependence of the kinetic term.

This choice of the regulator guarantees a supersymmetric RG trajectory; i.e., for a supersymmetric initial condition $\Gamma_{k\to\Lambda} \to S$, the solution to the flow equation Γ_k will remain manifestly supersymmetric for all k including the endpoint $\Gamma = \Gamma_{k\to 0}$. This does not only hold for the exact solution, but is also valid for truncated effective actions, provided the truncation is built from supersymmetric field operators.

V. LOCAL POTENTIAL APPROXIMATION

Various systematic and consistent approximation schemes for the construction of Γ_k can be devised with the flow equation. In this work, we use the derivative expansion which is based on the underlying assumption that the fully interacting theory remains sufficiently local if formulated in the given set of field variables. In order to preserve supersymmetry, we expand the effective action in powers of super-covariant derivatives in the off-shell formulation. This expansion allows for a systematic and unique classification of all possible operators. A truncation of the effective action to a finite derivative order leads to a closed set of equations for the expansion parameters.

In this section, we concentrate on the leading-order derivative expansion: the so-called local potential approximation. Here, the truncated effective Lagrangian is given by Eq. (11) with a scale-dependent superpotential W_k, such that the truncated effective action reads

$$\begin{aligned}\Gamma_k[\phi, F, \bar{\psi}, \psi] = \int d^2x \,\big(&\tfrac{1}{2}\partial_\mu\phi\partial^\mu\phi + \tfrac{i}{2}\bar{\psi}\not{\partial}\psi - \tfrac{1}{2}F^2 \\ &+ \tfrac{1}{2}W_k''(\phi)\bar{\psi}\gamma_*\psi - W_k'(\phi)F\big)\,.\end{aligned} \tag{29}$$

The derivation of the flow equation for the superpotential parallels the corresponding one for supersymmetric quantum mechanics given in a previous work [19]. Within the approximation of constant mean fields, the second functional derivative of the effective action plus regulator is

$$\begin{aligned}\Gamma_k^{(2)} + R_k &= \begin{pmatrix} A & W_k'''e_1 \otimes \bar{\psi}\gamma_* \\ W_k'''\gamma_*\psi \otimes e_1^T & B\end{pmatrix}, \\ e_1 &= (1,\,0)^T,\end{aligned} \tag{30}$$

where the operators on the diagonal read

$$\begin{aligned}A &= \begin{pmatrix} p^2(1+r_2) - FW_k''' + \tfrac{1}{2}W_k^{(4)}\bar{\psi}\gamma_*\psi & -W_k'' - r_1 \\ -W_k'' - r_1 & -1 - r_2\end{pmatrix}, \\ B &= i(1+r_2)\not{p} + \gamma_*(r_1 + W_k'').\end{aligned} \tag{31}$$

The inverse of the operator defined in Eq. (30) can be written as follows,

$$\begin{aligned}\frac{1}{\Gamma_k^{(2)} + R_k} &= \begin{pmatrix} G_k^{\mathrm{BB}} & G_k^{\mathrm{BF}} \\ G_k^{\mathrm{FB}} & G_k^{\mathrm{FF}}\end{pmatrix} \\ &= \begin{pmatrix} A^{-1} & 0 \\ 0 & B^{-1}\end{pmatrix} K \begin{pmatrix} A^{-1} & 0 \\ 0 & B^{-1}\end{pmatrix},\end{aligned} \tag{32}$$

where we have abbreviated

$$K = \begin{pmatrix} A + W_k'''^2(\bar\psi\gamma_* B^{-1}\gamma_*\psi)\, e_1 \otimes e_1^T & -W_k''' e_1 \otimes \bar\psi\gamma_* \\ -W_k'''\gamma_*\psi \otimes e_1^T & B - \frac{1}{2}W_k'''^2(e_1^T A^{-1} e_1)(\bar\psi\gamma_*\psi)\gamma_* \end{pmatrix}. \tag{33}$$

In order to verify that Eq. (32) is the inverse of Eq. (30), the Fierz identity $\psi \otimes \bar\psi = -\frac{1}{2}\gamma_*(\bar\psi\gamma_*\psi)$ is useful. This result is inserted into the flow equation (23), which in component notation reads

$$\partial_k \Gamma_k = \frac{1}{2}\,\mathrm{Tr}\left(\partial_k R_k^{\mathrm{B}}\, G_k^{\mathrm{BB}}\right) - \frac{1}{2}\,\mathrm{Tr}\left(\partial_k R_k^{\mathrm{F}} G_k^{\mathrm{FF}}\right). \tag{34}$$

The flow equation for $W_k'(\phi)$ is obtained by projecting both sides of this equation onto the term linear in the auxilary field. This yields

$$\partial_k W_k'(\phi) = -W_k''' \int \frac{d^2p}{4\pi^2}\left(\frac{(1+r_2)(W_k''+r_1)}{\Delta^2}\partial_k r_1 + \frac{p^2(1+r_2)^2 - (W_k''+r_1)^2}{2\Delta^2}\partial_k r_2\right), \tag{35}$$

where we have introduced $\Delta = p^2(1+r_2)^2 + (W_k''+r_1)^2$. Integrating with respect to ϕ and dropping an irrelevant constant leads to

$$\partial_k W_k(\phi) = \frac{1}{2}\int \frac{d^2p}{(2\pi)^2}\frac{(r_2+1)\partial_k r_1 - (r_1 + W_k''(\phi))\partial_k r_2}{\Delta}. \tag{36}$$

This flow equation for the superpotential has exactly the same structure as the corresponding flow equation in supersymmetric quantum mechanics [19]. This is not surprising since supersymmetric quantum mechanics can be obtained from this model through dimensional reduction.

Here we are interested in superpotentials for which the map $\mathbb{R} \ni \phi \to W'(\phi) \in \mathbb{R}$ has winding number zero as these potentials allow for dynamical supersymmetry breaking. For a polynomial W this is the case if W' tends asymptotically to an even power, $W'(\phi) \sim \mathrm{c}\,\phi^{2n}$. Then, the highest power of $W''(\phi)$ is odd. This implies that the mass-like regulator r_1 does not screen but merely shift possible zeroes of W_k''. Thus we may set $r_1 = 0$ without spoiling the IR properties of the flow.

In the present local-potential approximation, the simple cutoff function $r_2 = (k/|p| - 1)\,\theta(1 - p^2/k^2)$ turns out to be technically very convenient, since the momentum integration in Eq. (36) can be performed analytically,

$$\partial_k W_k(\phi) = -\frac{k}{4\pi}\frac{W_k''(\phi)}{k^2 + W_k''(\phi)^2}. \tag{37}$$

In order to calculate the bosonic potential $V(\phi) = \frac{1}{2}W'(\phi)^2$, we only need the derivative of the superpotential. The corresponding flow is

$$\partial_k W_k'(\phi) = -W_k'''(\phi)\frac{k}{4\pi}\frac{k^2 - W_k''(\phi)^2}{(k^2 + W_k''(\phi)^2)^2}. \tag{38}$$

This equation exhibits a particularity for any finite value of k, as the sign of the flow depends on whether $W_k''(\phi)^2$ is smaller or larger than k^2. For large ϕ, we generally expect both $(W_k'')^2$ and W_k''' to be large and positive for $\mathbb{Z}_2$ symmetric systems. In this case, the flow for large ϕ tends to deplete the height of the potential. Of course, for $\phi \to \infty$, we expect the denominator of Eq. (38) to win out over the numerator, such that the flow vanishes at large field amplitudes. For small ϕ, or, more generally, in the vicinity of local or global minima of W_k', there can be an inner domain where $(W_k'')^2 < k^2$. For convex potentials W_k' with $W_k''' > 0$, the flow is negative here, resulting in the tendency to flatten out this inner part of the potential W_k'. As the curvature W_k''' is related to the masses of the excitations, the flow shows a clear tendency to small masses if an inner domain with $(W_k'')^2 < k^2$ exists. As it will turn out later, this is a characteristic property of the supersymmetry-broken phase.

Let us note in passing that the regulator used in the present section can lead to artificial divergences at higher orders in the derivative expansion, e.g., when a wave function renormalization is included. Then a stronger regulator in the IR is needed; see, App. A for calculations at next-to-leading order in the derivative expansion.

VI. FIXED-POINT STRUCTURE

In this section, we investigate the fixed-point structure of the RG flow. We first concentrate on the local-potential approximation and later include next-to-leading-order terms in the derivative expansion. In fact, it turns out that there is a qualitative difference of the fixed-point superpotentials between the different orders. Similar observations are known from two-dimensional bosonic theories [34, 35] and are a particularity of two-dimensional systems. Still, the local-potential flow is interesting in its own right. Its IR flow is also quantitatively relevant for studies of the phase diagram, see Sect. VII.

Since RG fixed-point studies require a scaling form of the flow equation, we switch to dimensionless quantities w and t defined by $W_k(\phi) = k w_t(\phi)$ and $t = \ln(k/\Lambda)$. In two dimensions, a scalar field is dimensionless such that no dimensionful rescaling is required. The flow equation (37) for the dimensionless quantities reads

$$\partial_t w_t(\phi) + w_t(\phi) = -\frac{1}{4\pi}\frac{w_t''(\phi)}{1 + w_t''(\phi)^2} \tag{39}$$

with $\partial_t = k\partial_k$. The fixed points are characterized by $\partial_t w_*' = 0$. In the following, we solve the fixed-point equation by various methods.

A. Polynomial expansion

For small values of the field, a polynomial approximation for w_t' is justified. If $w_t'(\phi)$ is an even function at the cutoff scale then it remains even at all scales. Its expansion reads $w_t'(\phi) = \lambda_t(\phi^2 - a_t^2) + b_{4,t}\phi^4 + b_{6,t}\phi^6 + b_{8,t}\phi^8 + \ldots$. The dimensionless couplings $\lambda_t, b_{t,i}$ relate to the bare couplings $\bar{\lambda}, \bar{b}_i$ through $\bar{\lambda} = k\lambda_t$ and $\bar{b}_i = k b_{t,i}$. $\bar{a}$ is dimensionless, therefore we have $\bar{a} = a_t$.

Expanding both sides of the flow equation in terms of ϕ, a comparison of coefficients leads to the following system of coupled ordinary differential equations:

$$\begin{aligned}
\partial_t a_t^2 =& \frac{1}{2\pi} - \frac{6\lambda_t^2 \cdot a_t^2}{\pi} + a_t^2 \frac{3b_{4,t}}{\pi\lambda_t} \\
\partial_t \lambda_t =& -\frac{3b_{4,t}}{\pi} + \frac{6\lambda_t^3}{\pi} - \lambda_t \\
\partial_t b_{4,t} =& -\frac{15b_{6,t}}{2\pi} + \frac{60b_{4,t}\cdot\lambda_t^2}{\pi} - \frac{40\lambda_t^5}{\pi} - b_{4,t} \\
\partial_t b_{6,t} =& -\frac{14b_{8,t}}{\pi} - \frac{560b_{4,t}\lambda_t^4}{\pi} + \frac{168b_{4,t}^2\lambda_t}{\pi} \\
&+ \frac{126b_{6,t}\lambda_t^2}{\pi} + \frac{224\lambda_t^7}{\pi} - b_{6,t} \\
&\vdots \\
\partial_t b_{2n,t} =& -\frac{(n+1)(n+2)}{4\pi} b_{n+2,t} + f_{2n}\left(\lambda_t, b_{4,t}, \ldots, b_{2n,t}\right).
\end{aligned} \tag{40}$$

Note that only w'' enters the right-hand side of the flow equation (39); in particular, the lowest coupling constant a_t^2 does not enter the equations for the higher order couplings.

At a fixed point, the coupling constants, marked by an asterisk, become scale invariant such that the left-hand sides in Eq. (40) vanish. The corresponding system of equations

$$b_{2n+2}^* = \frac{4\pi}{(n+1)(n+2)} f_{2n}\left(\lambda^*, b_4^*, \ldots, b_{2n}^*\right) \tag{41}$$

can be solved iteratively due to the triangular form of the system of flow equations (40). At a fixed point, b_{2n}^* is a polynomial of order $2n+1$ in λ^*. Because of the $\mathbb{Z}_2$ symmetry of the system of equations, these polynomials are odd. In particular, $b_4^*(\lambda^*) = 2\lambda^{*3} - \pi\lambda^*/3$ such that the projection of any fixed-point solution on the subspace defined by the couplings λ^* and b_4^* fall onto the curve $b_4^*(\lambda^*)$ depicted in Fig. 2. Inserting $b_4^*(\lambda^*)$ into the first equation in (40) yields $(a^*)^2 = 1/2\pi$. Later, we shall see that a_t^2 defines an IR unstable direction near a fixed point.

Let us truncate the polynomial expansion of the flow equation for w_t and keep only terms up to order ϕ^{2n+1} in (39). This is equivalent to keeping the lowest n fixed point equations which yield $b_{2m}^*(\lambda^*)$ for $m \leq n$. In the nth equation, the higher-order coupling b_{2n+2} occurs

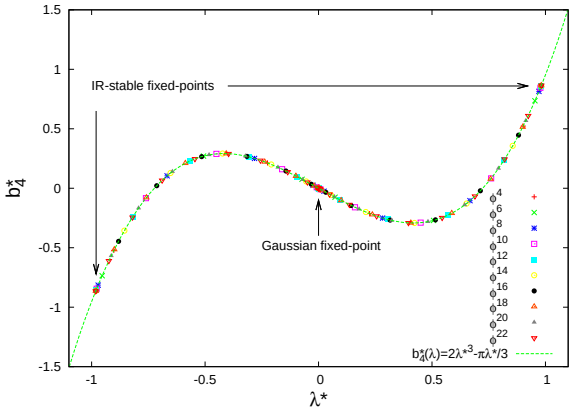

FIG. 2: Projection of the coefficients of all fixed points for different truncations on the plane of the couplings λ and b_4.

which we set to zero at the fixed point, $b_{2n+2}^* = 0$.[1] This leads to the polynomial equation

$$f_{2n}(\lambda^*) = f_{2n}\left(\lambda^*, b_4^*(\lambda^*), \ldots, b_{2n}^*(\lambda^*)\right) = 0, \tag{42}$$

where the solutions $b_{2m}^*(\lambda^*)$ are to be inserted. With MATHEMATICA, we have checked up to order $2n = 22$ that all $2n+1$ roots of the odd polynomial $f_{2n}(\lambda^*)$ of order $2n+1$ are real.

Due to the underlying $\mathbb{Z}_2$ symmetry, the remaining fixed points of the truncated system come in pairs $\pm(\lambda^*, b_4^*, \ldots, b_{2n}^*)$. Hence, we find n independent nontrivial solutions to the fixed-point equations in addition to the Gaußian fixed point where all couplings vanish. As discussed in the next subsection, only one of these solutions belongs to an infrared stable fixed point with all but one eigenvalues in the stability matrix being positive (i.e., all but one critical exponents being negative). It turns out that this infrared-stable fixed point corresponds to the largest root of Eq. (42), as indicated in Fig. 2. With increasing order of the polynomial truncation the root belonging to the IR-stable fixed point converges to $\lambda_{\rm crit} \simeq 0.9816$. Roots belonging to any other fixed point are bounded by

$$-\lambda_{\rm crit} < \lambda^* < \lambda_{\rm crit}. \tag{43}$$

In Fig. 3 (left panel), we have plotted the values for the two lowest coefficients λ^* and b_4^* at the infrared-stable fixed point in the polynomial expansion for different orders of truncations. We observe a rapid convergence with increasing order of the polynomial approximation. This suggests that the polynomial approximation to the superpotential in the local potential approximation has acceptable convergence properties.

[1] This prescription is not unique. Alternatively, we could set b_{2n+2}^*, for instance, equal to its perturbative one-loop value. In any case, the choice $b_{2n+2}^* = 0$ used here is self-consistent in the sense that the equations of $b_{\leq 2n}$ are closed and do not depend on further input.

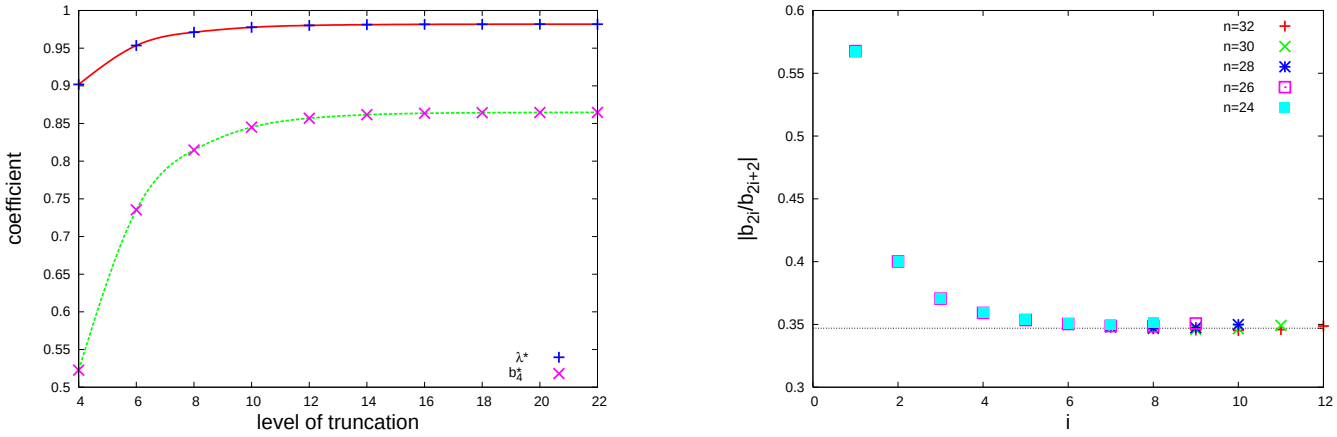

FIG. 3: Left panel: The first two coefficients λ and b_4 of the IR stable fixed point for different truncations. Right panel: Ratio of successive couplings of the IR-stable fixed point yielding an estimate of the radius of convergence.

	coefficients at IR-fixed point						
$2n$	λ^*	b_4^*	b_6^*	b_8^*	b_{10}^*	b_{12}^*	b_{14}^*
2	0.7236						
4	0.9019	0.5227					
6	0.9535	0.7354	0.8372				
8	0.9711	0.8148	1.199	1.694			
10	0.9777	0.8451	1.345	2.420	3.801		
12	0.9802	0.8570	1.402	2.716	5.401	9.030	
14	0.9812	0.8617	1.425	2.836	6.054	12.77	22.23

TABLE I: The coefficients of the IR-stable fixed point potential for different truncations.

In Fig. 3 (right panel), we have plotted the inverse ratio of successive couplings at the infrared-stable fixed point for increasing truncation order. This facilitates an estimate of the radius of convergence for a series expansion of w'_* in powers of ϕ^2,

$$r_{\rm con}^2 = \lim_{i\to\infty} \left| \frac{b_{2i}^*}{b_{2i+2}^*} \right|.$$

An extrapolation leads to the approximate value $r_{\rm con}^2 \simeq 0.35$ such that for $|\phi| < r_{\rm con}$ the polynomial $\lambda^*(\phi^2 - a^2) + \sum_2^n b_{2m}^* \phi^{2m}$ converges to the IR-stable fixed point solution w'_*. In Table I, the coefficients in the polynomial approximations to w'_* at the IR-stable fixed point are listed. Note that the fixed-point values are generically regulator dependent, and thus are not directly related to physical quantities.

1. *Stability analysis and critical exponents*

Whereas the values of the fixed-point couplings are regulator dependent, the *critical exponents* are universal and give rise to a classification of the fixed points. The critical exponents are defined as the negative eigenvalues θ^I of the stability matrix at the fixed point,

$$B_i{}^j = \left. \frac{\partial(\partial_t b_i)}{\partial b_j} \right|_{b=b^*}, \quad B_i{}^j v_j^I = -\theta^I v_i^I, \tag{44}$$

where we have set $b_0 = a_t^2$, $b_2 = \lambda$, and I labels the different critical exponents θ^I and eigendirections v_i^I. Critical exponents with positive real part correspond to RG relevant directions, whereas exponents with negative real part mark irrelevant directions. Inserting the flow of λ_t into that of a_t^2, cf. Eq. (40), we obtain

$$\partial_t a_t^2 = \frac{1}{2\pi} - a_t^2 - \frac{a_t^2}{\lambda_t} \partial_t \lambda_t. \tag{45}$$

We observe that the 00-component of the stability matrix at any fixed-point yields, $B_0{}^0 = -1$. This together with the fact that the remainder of the first column vanishes, $B_{i\geq 1}{}^0 = 0$, implies that a_t^2 is always an eigendirection of $B_i{}^j$ with corresponding critical exponent $\theta^0 = 1$. Note that this result is manifestly regulator independent and thus universal. We conclude that any fixed point of the superpotential in the local-potential approximation has at least one RG relevant direction. In analogy with potential flows near the Wilson-Fisher fixed point of Ising-like systems, we introduce the following notion for the leading critical exponent corresponding to this relevant direction:

$$\nu_W = \frac{1}{\theta^0} = 1. \tag{46}$$

Even though ν_W plays the same role for the superpotential flow as the critical exponent ν does for the potential flow in Ising-like systems, it should be stressed that ν_W does not correspond to the scaling exponent of the correlation length (as ν does in Ising-like systems). We will later see that ν_W quantifies certain properties of the phase diagram.

Depending on whether we study the UV or IR flow of the system, the fixed points have a different meaning.

λ^*	Critical exponents θ^I							
$\pm.9816$	-1.54	-7.43	-18.3	-37.3	-68.9	-120	-204	-351
$\pm.8813$	6.16	-1.64	-9.82	-25.6	-52.5	-96.9	-170	-300
$\pm.7131$	21.4	4.37	-1.57	-11.1	-30.1	-63.3	-120	-223
$\pm.5152$	28.7	13.3	3.33	-1.39	-11.6	-32.8	-71.7	-145
$\pm.3158$	$20.0 - 4.55$ i	$20.0 + 4.55$ i	8.40	2.57	-1.14	-11.6	-34.3	-80.4
$\pm.1437$	$11.2 + 9.02$ i	$11.2 - 9.02$ i	8.63	5.19	1.95	$-.842$	-11.1	-35.7
$\pm.0322$	$4.20 + 1.18$ i	$4.20 - 1.18$ i	2.86	$2.72 + 6.47$ i	$2.72 - 6.47$ i	1.47	$-.540$	-10.5
$\pm.0003$	$1.57 + .125$ i	$1.57 - .125$ i	$1.43 + .702$ i	$1.43 + .702$ i	1.14	$.542 + .982$ i	$.542 + .982$ i	-0.221
0	1	1	1	1	1	1	1	1

TABLE II: Critical exponents θ^I (negative eigenvalues of the stability matrix) for a polynomial truncation at $2n = 16$ for the nine different fix points in the local-potential approximation. The first exponent $\theta^0 = 1$ which is common to all fixed points is not shown here.

Towards the UV, any of the fixed points which we have found can be used to define a UV completion of the model in the sense of Weinberg's asymptotic safety scenario [36]. All relevant directions emanating from the fixed point span the critical hypersurface. The dimensionality of this critical surface, i.e., the number of critical exponents with $\mathrm{Re}\,\theta^I \geq 0$, corresponds to the number of physical parameters which have to be fixed in order to unambiguously define the flow towards the IR.[2] Once these initial conditions to the flow are provided, any other quantity or correlation function can be predicted within the theory. Since $\theta^0 = 1$, we conclude that any UV completion has at least one physical parameter.

Within the local-potential approximation at order $2n = 16$ of the polynomial expansion, the critical exponents $\theta^{I\geq 1}$ are given in Table II for all 17 fixed-point potentials. By using a different regulator, we check in App. B that the regulator dependence of the relevant positive critical exponents is rather small (up to 10% or much less), which confirms the reliability of the present truncation. Classifying the fixed-point potentials by the slope λ^* of the potential w_t' as a function of ϕ^2 at $\phi^2 = 0$, the number of relevant directions increases as the slope $|\lambda^*|$ decreases. The different fixed-point potentials in the local-potential approximation – if they persist to higher truncation orders – thus correspond to different UV completions of the present system with increasing physical parameters. These different UV completions thus define different nonperturbatively renormalized Wess-Zumino models in two-dimensions.

As for the flow towards the IR, the fixed points can generically be related with critical points in the phase diagram of the system. Since the relevant directions are IR repulsive, fine-tuning the relevant direction to the fixed point corresponds to tuning the system onto its critical point. In this sense, the relevant direction corresponding to a_t^2 with $\nu_W = 1/\theta^0 = 1$ is similar to the temperature parameter in Ising-like systems (or a mass parameter in O(N)-type relativistic models). For instance, in the domain of attraction of the maximally IR-stable fixed point with only a_t^2 as relevant direction, the tuning of a_t^2 distinguishes between the supersymmetric and symmetry-broken phases of the model. More generally, if a system is in the domain of attraction of a fixed-point with N relevant directions, the phases of broken and unbroken supersymmetry are separated by an N-dimensional hypersurface in the space of couplings.

There is one important difference to Ising-like systems: the coupling a_t^2 associated with the one common relevant direction does not feed back into the flow of the higher-order couplings. Therefore, the remaining couplings are attracted towards the maximally IR-stable fixed point for any regular trajectory irrespective of the flow of a_t^2.[3] We conclude that the maximally IR-stable fixed point governs the flow towards the IR of $w_t''(\phi)$ in the domain, where the polynomial expansion is valid.

Let us finally mention that the critical exponent $\nu_W = 1/\theta^0 = 1$ receives corrections at higher orders in the derivative expansion, cf. Eq. (57). Still the relevance of the maximally IR-stable fixed point for the IR flow of the potential persists.

In Table III, we collected the eigenvalues (negative critical exponents) for the maximally IR-stable fix point for different truncations.

B. Solving of the nonlinear differential equation

For large values of the scalar field, the polynomial truncation is not valid anymore. Hence, we consider here the full nonlinear ordinary differential equation that de-

[2] For marginal directions with $\mathrm{Re}\,\theta^I = 0$, the flow in the fixed-point regime has to be studied beyond linear order. Depending on the sign of the first non-vanishing order, these directions are again either marginally relevant or irrelevant.

[3] Irregular trajectories can run to infinity at a finite value of k. These divergences are either physically meaningless or signal the breakdown of the truncation.

$2n$	λ^*	eigenvalues of the stability matrix						
4	±0.9019						16.35	1.846
6	±0.9535					42.32	12.00	1.716
8	±0.9711				79.83	30.67	9.951	1.635
10	±0.9777			129.1	58.61	25.05	8.794	1.588
12	±0.9802		190.6	96.49	47.97	21.75	8.101	1.561
14	±0.9812	264.5	144.8	79.50	41.51	19.67	7.680	1.546
16	±0.9816	351.2	204.1	120.3	68.90	37.25	18.30	7.427	1.539

TABLE III: Eigenvalues of the stability matrix (negative critical exponents) of the maximally IR-stable fix point for different polynomial truncations in the local-potential approximation. The first exponent $\theta^0 = 1$ is not shown here. For the first subleading exponent (last column), the polynomial expansion shows a satisfactory convergence.

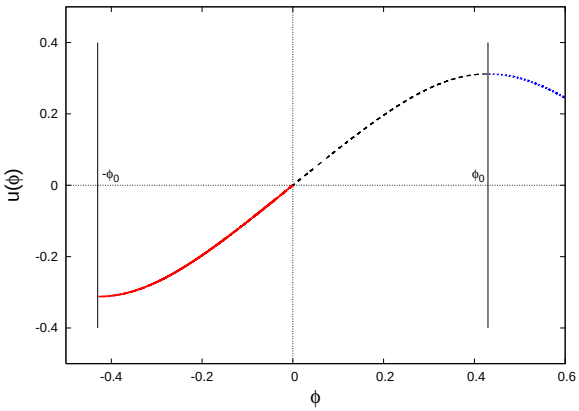

FIG. 4: Illustration of the discussion of oscillating solutions, see text.

scribes the fixed point potential in the local-potential approximation. In the polynomial approximation, the potential w_t and w_t' contain the IR-unstable coupling a_t which does not flow into the fixed point. Upon differentiation of the fixed-point equation for $w_*'(\phi)$,

$$w_*' = -\frac{w_*'''}{4\pi}\frac{1-w_*''^2}{(1+w_*''^2)^2}, \tag{47}$$

with respect to ϕ, we arrive at the following fixed-point equation for the a_*-independent function $w_*''(\phi) \equiv u(\phi)$,

$$(1-u^4)u'' = 2u'^2\,(3-u^2)\,u - (1+u^2)^3\,4\pi u. \tag{48}$$

Since a_t^2 does not appear in Eq. (48), we expect to find a fully IR-stable solution to this nonlinear differential equation (in addition to further solutions with IR unstable directions).

As before, we consider odd solutions $u(\phi)$ which are fixed by the initial conditions $u(0) = 0$ and a finite value for $u'(0)$. In fact, we find a continuum of oscillatory solutions that are defined for all values of ϕ. In addition, we identify solutions that hit the singular line $u(\phi) = 1$ of the differential equation (48) but can be continued without cusps. Solutions of the second class exist only in a finite ϕ range.

1. *Oscillating solutions*

Let us integrate the fixed-point equation (48) with initial conditions at $-\phi_0 < 0$ (see Fig. 4):

$$u(-\phi_0) = u_0, \quad u'(-\phi_0) = 0 \quad \text{where} \quad -1 < u_0 < 0.$$

The initial point is an extremum of the solution. The differential equation (48) implies that this extremum is indeed a minimum such that u approaches the ϕ axis away from $-\phi_0$. Actually it must intersect the axis at some point. Otherwise, it would possess a maximum at some ϕ_1 with $u(-\phi_0) < u(\phi_1) < 0$ or it would monotonically approach the ϕ axis without crossing it. But a maximum with $-1 < u(\phi_1) < 0$ contradicts the differential equation (48) which implies that $u''(\phi_1) > 0$. Also, if u approached the ϕ axis monotonically from below then near the axis the differential equation would imply $u'' \approx -4\pi u > 0$. Therefore, the slope of u would increase with increasing ϕ such that finally u would intersect the ϕ axis.

We conclude that u must intersect the ϕ axis and we may assume that this happens at $\phi = 0$, such that the solution starts off at the minimum at $-\phi_0 < 0$ and hits the axis at the origin. This solution extends to an odd solution owing to the symmetry $u(\phi) \to -u(-\phi)$ of the differential equation and hence has a maximum at $\phi_0 > 0$ with $0 < u(\phi_0) = -u(-\phi_0) < 1$. Because of the translational invariance $\phi \to \phi + c$ and the symmetry $u(\phi) \to u(-\phi)$ of the fixed point equation the solution must be symmetric relative to ϕ_0, i.e. $u(\phi_0 - \phi) = u(\phi_0 + \phi)$. This proves that every solution with $-1 < u(\text{extrema}) < 1$ is periodic and takes its values between -1 and 1. The lines $u(\phi) = \pm 1$ repel solutions oscillating in the strip $-1 < u < 1$ as long as the slope $u'(0) = \gamma$ is less than $\gamma_{\rm crit} \simeq 1.964$. Solutions with $\gamma \geq \gamma_{\rm crit}$ hit the singularity at $u = 1$.

In a similar fashion, one argues that there exists a second class of solutions of the differential equation having just one minimum with $u > 1$ or having just one maximum with $u < -1$. Solution in this class are not periodic and never hit the singular line $u = \pm 1$. Since they cannot be continuous and antisymmetric they are discarded.

2. *Comparison with the polynomial expansion*

In the preceding subsection, we have seen in the polynomial expansions of the truncated system that the slope $\gamma = 2\lambda$ is bounded by $2\lambda_{\rm crit} \simeq 1.964$. This is just the critical value $\gamma_{\rm crit}$ for the existence of oscillating solutions of the fixed point equation (48). We conjecture that a polynomial solution belonging to a fixed point with two or more relevant directions of the truncated systems, corresponding to a non-maximal root of f_{2n} in (42), converges

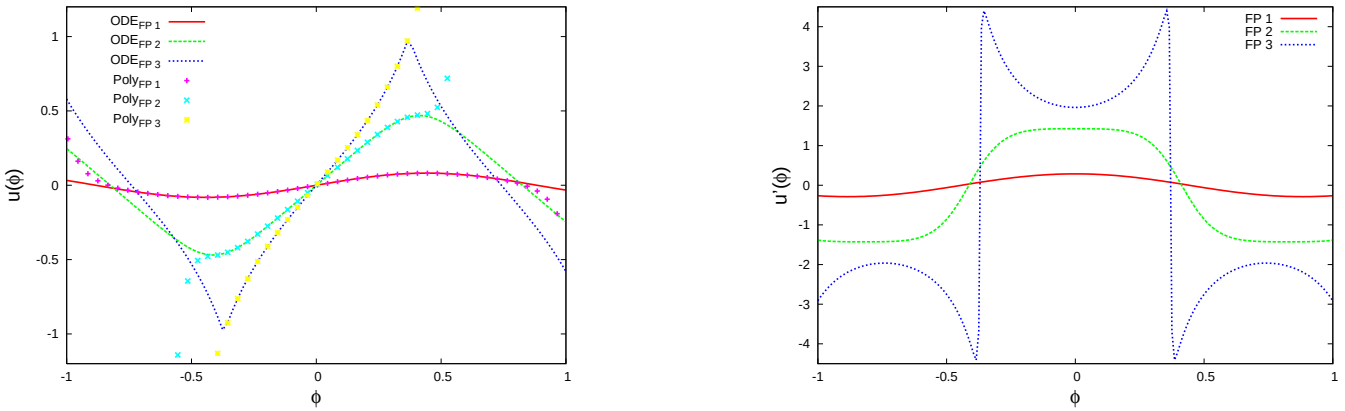

FIG. 5: *Left panel:* Comparison between the numerical solution to the differential equation (ODE) and the polynomial approximation (Poly) to 16th order for three different fixed points. The fixed points FP1, FP2, and FP3 have the initial slope $\gamma = 0.287, 1.4262$ and 1.963. The fixed point FP3 is the maximally IR-stable fixed-point. *Right panel:* The first derivative of the potentials in Fig. 5.

to the Taylor series of an oscillating solution. In Fig. 5 (left panel), we have plotted three full numerical solutions and the corresponding polynomial approximation truncated at ϕ^{16} with the same initial value $\gamma = 2\lambda$. For the first half period, we find an excellent agreement between polynomial approximation and numerical solution.

3. *Solution with $u(\phi) = 1$ for some field value ϕ*

Regular periodic solutions only exist for $-\gamma_{\rm crit} < \gamma < \gamma_{\rm crit}$. Increasing the slope at the origin gradually from 0 to $\gamma_{\rm crit}$, the value $u(\phi_{\rm max})$ at the maximum approaches the singular line $u = 1$ and finally hits the singularity at the critical field $\phi_{\rm crit} \simeq 0.3704$. At the same time the curvature at the maximum tends to $-\infty$. With increasing order the IR stable fixed points for the polynomial truncations converge to the Taylor expansion of the solution with the critical slope $\gamma_{\rm crit}$.

In order to study the solutions near the singular line, we insert the Taylor expansion $u(\phi_{\rm crit} + \delta\phi) = u(\phi_{\rm crit}) + a_1\delta\phi + a_2\delta\phi^2/2 + \dots$ with $u(\phi_{\rm crit}) = 1$ and compare coefficients. One sees that the expansion coefficients are finite if $a_1 = u'(\phi_{\rm crit}) = \pm\sqrt{8\pi}$. If this condition is not met, the solution hits the singular line $u(\phi) = 1$ with infinite slope, as can be seen by studying the differential equation for the inverse function $\phi(u)$. The behavior of a solution depends in an essential way on γ: if the initial slope is less than $\gamma_{\rm crit}$ then the solution is smooth and periodic, if the initial slope is $\gamma_{\rm crit}$ then it hits the singular line $u(\phi) = 1$ with slope $\sqrt{8\pi}$ and if the initial slope is bigger than $\gamma_{\rm crit}$ then the solution hits the singular line vertically; see Fig. 6. If we viewed the solutions hitting the singular line as parametric continuation of the periodic solutions as γ approaches $\gamma_{\rm crit}$, we would reflect the solution at the singular line, similarly to the solution FP3 in Fig. 5, left panel. For the maximally IR-stable fixed-point solution with initial slope $\gamma_{\rm crit}$ the slope at $\phi_{\rm crit}$ would then jump from $\sqrt{8\pi}$ to $-\sqrt{8\pi}$, as shown in Fig. 5, right panel, where we depicted the function $u'(\phi) = w'''(\phi)$ for three different values of the initial slope $\gamma = 2\lambda$.

However, there is a way to extend the solutions hitting the singular line without cusps. To see this more clearly we note that $v = 1/u$ fulfills almost the identical fixed-point equation as u,

$$(1 - v^4)v'' = 2v'^2\,(3 - v^2)\,v - 4\pi(1 + v^2)^3/v. \qquad (49)$$

Upon approaching the singular line $u \to 1$ and $v \to 1$, the two equations (48) and (49) become identical. This implies that near the singular line the reflection at the singular line maps solutions into solutions. Thus, all solutions with $\gamma \geq \gamma_{\rm crit}$ hitting the singular line vertically or with slope $\sqrt{8\pi}$ can be extended without cusps beyond the singular line.

We have studied these solutions for large values $u \gg 1$. It is not difficult to see that there exist no solutions with $u \sim \phi^\alpha$ for large ϕ. (This will become different at next-to-leading order in the derivative expansion.) We find the asymptotic solution

$$u_{\rm as}(\phi) = e^{{\rm erf}^{-1}\left(\pm 2\sqrt{2}\, e^{-\frac{c_1}{8\pi}(\phi + c_2)}\right)^2 - \frac{c_1}{8\pi}} \qquad (50)$$

with $c_1 \simeq -20.02$ and $c_2 \simeq -0.423$ for the maximally IR-stable fixed point extended without cusp beyond the singular line. It is finite only for

$$-\phi_{{\rm crit},2} < \phi < \phi_{{\rm crit},2}, \quad \phi_{{\rm crit},2} = 0.5823. \qquad (51)$$

An unbounded and cusp-free fixed point solution belongs to a field theory with compact target space.

Let us summarize our findings. As a regular oscillating or a non-differentiable bouncing solution $u(\phi)$ is finite for all values of the field, this implies a vanishing *dimensionful* $W_k''(\phi) = ku(\phi)$ as the scale k is lowered to the infrared. The solutions which penetrate the singular line

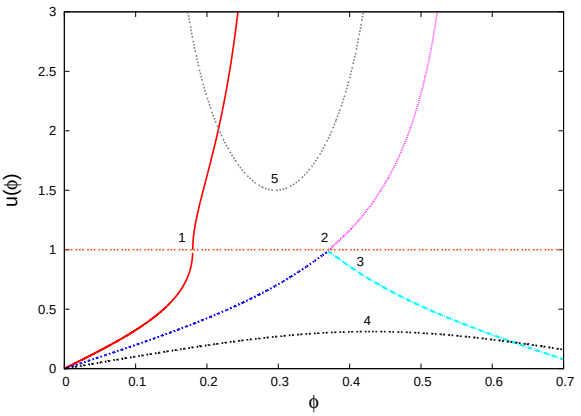

FIG. 6: All types of possible solutions to the fixed-point differential equation in local-potential approximation: (1) $\gamma > \gamma_{\rm crit}$, (2) $\gamma = \gamma_{\rm crit}$, finite ϕ range, (3) $\gamma = \gamma_{\rm crit}$, oscillating solution, (4) $\gamma < \gamma_{\rm crit}$, oscillating solution, (5) solution with just one extremum

$u = 1$ without a cusp are unbounded from below and above and confine the field to a finite interval. The different types of solutions are depicted in Fig. 6.

C. Fixed points at next-to-leading order in the derivative expansion

1. *Next-to-leading-order flows*

Two dimensional scalar field theories and their supersymmetric extensions exhibit infinitely many scale invariant fixed-points characterized by the central charge c of a conformal field theory [37]. In the local potential approximation to scalar field theories, only periodic, sine-Gordon type fixed-point solutions are accessible. At next-to-leading order in the derivative expansion, one finds additional non-periodic fixed-point solutions [34, 35]. Here we find analogous results for the two-dimensional Wess-Zumino model.

In this subsection, we consider fixed point solutions with scale-dependent but field-independent wave function renormalization Z_k in the next-to-leading order approximation. The corresponding flow equations are derived in appendix A. The full next-to-leading-order approximation would include a field-dependent wave function renormalization $Z_k(\Phi)$. For supersymmetric quantum mechanics, this order has been computed in [19]. Here, we confine ourselves to the simpler approximation $Z_k(\Phi) \to Z_k(0) \equiv Z_k$.

Let us introduce renormalized fields χ, by rescaling ϕ with the wave function renormalization $\phi \to \chi = Z_k\phi$. This implies a dimensionless renormalized superpotential $\mathfrak{w}_t(\chi) = W_k(\chi/Z_k)/k$. The calculation of the flow is outlined in App. A; in order to avoid artificial IR singularities, different regulator shape functions were used in comparison with the local-potential approximation: $r_1 = 0$ and $r_2 = (k^2/p^2 - 1)\theta(1 - p^2/k^2)$. For the rescaled quantities, the flow equations read

$$\partial_t \mathfrak{w}_t' + \mathfrak{w}_t' - \frac{\eta}{2}(\chi \mathfrak{w}_t')' = \frac{1}{4\pi}\frac{\mathfrak{w}_t'''}{\mathfrak{w}_t''^2} \times \left[\ln\left(1+\mathfrak{w}_t''^2\right)\left(1 - \frac{\eta}{2}\frac{3+\mathfrak{w}_t''^2}{\mathfrak{w}_t''^2}\right) - \frac{2\mathfrak{w}_t''^2}{1+\mathfrak{w}_t''^2} + \frac{3\eta}{2}\right], \tag{52}$$

$$\eta := -\,\partial_t \ln Z_k^2 = \frac{1}{4\pi}\left(\frac{\mathfrak{w}_k'''}{\mathfrak{w}_k''^2}\right)^2 \times \left[\frac{\eta\,\mathfrak{w}_k''^2}{1+\mathfrak{w}_k''^2} - \eta \ln\left(1+\mathfrak{w}_k''^2\right) + \frac{2\mathfrak{w}_k''^4}{(1+\mathfrak{w}_k''^2)^2}\right]_{\chi=0}, \tag{53}$$

where we have dropped the arguments in $\mathfrak{w}_t(\chi)$ for simplicity. Since the anomalous dimension is assumed to be constant in this approximation, we have projected Eq. (53) onto $\chi = 0$. Note that the limit $\mathfrak{w}_t''(0) \to 0$ of the right-hand side of Eq. (53) exists, yielding

$$\eta = \frac{4\lambda^2}{\lambda^2 + 2\pi}. \tag{54}$$

2. *Polynomial expansion and superscaling relation*

The polynomial expansion of the next-to-leading-order superpotential flow equation in terms of dimensionless renormalized couplings is given in App. A. For instance, the flow of the renormalized parameter a_t^2 can be written as (cf. Eq. (A12))

$$\partial_t a_t^2 = \frac{1}{2\pi}\left(1 - \frac{\eta}{4}\right) - \left(1 - \frac{\eta}{2}\right)a_t^2 - \frac{a_t^2}{\lambda_t}\,\partial_t \lambda_t, \tag{55}$$

which is the next-to-leading-order analogue of Eq. (45). The renormalized couplings are related to their unrenormalized analogues by

$$\lambda_t = \frac{1}{k}\frac{1}{Z_k^3}\,\bar{\lambda}_k, \quad a_t^2 = Z_k^2 \bar{a}_k^2. \tag{56}$$

Similarly to the local-potential approximation, we observe that the 00-component of the stability matrix at any fixed point yields $B_0{}^0 = -(1 - \frac{\eta}{2})$, where $\eta = \eta^*$ has to be evaluated at the corresponding fixed point. Since the remainder of the first column vanishes, $B^0_{i\geq 1} = 0$, the coupling a_t^2 remains always an eigendirection of $B_i{}^j$ at any fixed point with a critical exponent $\theta^0 = -(1 - \frac{\eta}{2})$, implying a *superscaling relation*

$$\nu_W \equiv \frac{1}{\theta^0} = \frac{2}{2-\eta}, \tag{57}$$

where we have again introduced an Ising-like notation for the critical exponent of the superpotential associated with the a_t^2 direction. This is a remarkable relation as it relates this superpotential exponent with the anomalous dimension. Recall that in Ising-like systems the thermodynamic main exponents (i.e., α, β, γ and δ) are related

$2n$	2	4	6	8	10	12	14
η	0.3284	0.4194	0.4358	0.4386	0.4388	0.4387	0.4386
$1/\nu_W$	0.8358	0.7903	0.7821	0.7807	0.7806	0.78065	0.7807

TABLE IV: Numerical verification of the superscaling relation (57): anomalous dimension η and the critical exponent $1/\nu_W$ of a^2 for increasing orders in a polynomial truncation evaluated for the maximally IR-stable fixed-point.

among each other by scaling relations, and can be deduced from the correlation exponents ν and η by hyperscaling relations. Beyond that there is no general relation between ν and η. The superscaling relation (57) thus represents a special feature of the present supersymmetric model.

We would like to stress that Eq. (57) is an exact relation to next-to-leading order in the supercovariant derivative expansion of the effective action. In particular, the inclusion of a field-dependent $Z_k(\phi)$ implying $\eta \to \eta(\phi)$ does not modify the superscaling relation, since the superscaling relation arises from the expansion in ϕ near $\phi = 0$. Beyond next-to-leading order, Eq. (57) might, in fact, receive corrections, since higher-derivative operators can still take influence on the flow of the superpotential mediated by higher-order interactions between the scalar field and the auxiliary field. Whether or not these interactions play a role for the superscaling relation at the fixed points needs to be clarified by future studies.

Within the present next-to-leading-order truncation, a numerical determination of the critical exponents from the full set of polynomially expanded flow equations, of course, confirms the superscaling relation to a high accuracy. Numerical values for η and ν_W at the maximally IR-stable fixed point for increasing order of polynomial truncations are given in Table IV. We also observe a rapid convergence of the polynomial expansion, yielding our best estimates $\eta \simeq 0.4386$ and $1/\nu_W \simeq 0.7807$ for the critical exponents at the maximally IR-stable fixed point. As the anomalous dimension is comparatively large, we expect significant quantitative corrections to arise from higher orders in the derivative expansion.

As discussed below, the superscaling relation has an immediate physical consequence for the IR flow of the masses in the supersymmetry broken phase.

3. *Fixed points of the nonlinear superpotential flow at next-to-leading order*

In order to go beyond the polynomial expansion, let us first study the asymptotic behavior of the right-hand side of the flow equation (52):

$$\mathfrak{w}_t''^2 \to 0 : \frac{\eta-4}{16\pi}\,\mathfrak{w}_t''' \quad \text{and} \tag{58}$$

$$\mathfrak{w}_t''^2 \to \infty : \frac{2-\eta}{8\pi}\,\frac{\mathfrak{w}_t'''}{\mathfrak{w}_t''^2}\,\ln(1+\mathfrak{w}_t''^2). \tag{59}$$

It turns out to be a self-consistent assumption that these asymptotic right-hand sides are subdominant in comparison with the left-hand side of Eq. (52) at a fixed point $\partial_t \mathfrak{w}_*' = 0$ both for small and large values of χ. From this, it follows that $\mathfrak{w}_*'$ is proportional to $\chi^{2/\eta-1}$ for large $\mathfrak{w}_*''$. In particular, $\mathfrak{w}_*'$ grows faster than any polynomial for $\eta = 0$, in complete agreement with our previous results in section VI.

Now, for a non-vanishing η we find a new class of solutions. For these new solutions, we consider again the derivative of Eq. (52). This leads to the following fixed point equation for $u = \mathfrak{w}_*''$ (note that u now contains a wave function renormalization in contrast to section VI):

$$\begin{aligned}
&\frac{u''}{4\pi}\left[\left(\frac{\eta(3+u^2)}{2u^4}-\frac{1}{u^2}\right)\ln\left(1+u^2\right)+\frac{2}{1+u^2}-\frac{3\eta}{2u^2}\right]\\
&=(\eta-1)u+\frac{\eta\chi}{2}u'+\frac{u'^2}{2\pi}\left[\frac{1+3u^2}{u(1+u^2)^2}-\frac{\eta(3+2u^2)}{u^3(1+u^2)}\right.\\
&\quad\left.+\left(\frac{\eta(6+u^2)}{2u^5}-\frac{1}{u^3}\right)\ln\left(1+u^2\right)\right].
\end{aligned} \tag{60}$$

For an initial condition in terms of an odd superpotential W_Λ at the UV scale $k = \Lambda$, $\mathfrak{w}_t$ is odd and the fixed point solution $u = \mathfrak{w}_*''$ vanishes at the origin. Thus for weak fields we have $u(\chi) \ll 1$ and we may expand the logarithm in powers of u. The resulting fixed point equation for small u is regular for $u \to 0$ and reads

$$\begin{aligned}
&\frac{u''}{16\pi}\left((\eta-4)+(6-\eta)u^2+\frac{5}{6}(\eta-2)u^4+\dots\right)\\
&=-\frac{uu'^2}{8\pi}\left((6-\eta)+\frac{5}{3}(\eta-8)u^2+\frac{21}{10}(10-\eta)u^4+\dots\right)\\
&\quad-\frac{\eta}{2}\chi u'-(\eta-1)u.
\end{aligned} \tag{61}$$

Following [34], we first consider η in Eq. (60) as a free parameter. The initial conditions $u(0) = 0$ and $u'(0) = \gamma = 2\lambda$ are parameterized by the slope γ at the origin. A solution of Eq. (60) with generic slope will run into a singularity because the factor multiplying u'' eventually becomes zero. By fine-tuning the slope it is possible to find regular solutions for a given value of η. In Fig. 7 (left panel) we show three regular potentials for $\eta = 0.1$. For large values of χ, they behave like $\mathfrak{w}''(\chi) \sim \chi^{18}$.

These regular solutions define curves of fixed-point solutions in the γ-η plane. This is shown in Fig. 7 (right panel). For $\eta = 2/3$ we find a potential that behaves as $u \sim \chi$ in the asymptotic region. We do not find solutions with larger values for η. For $0 < \eta < 2/3$ it follows from simple monotony arguments that the factor multiplying $\mathfrak{u}''$ in Eq. (60) has only one node at some value

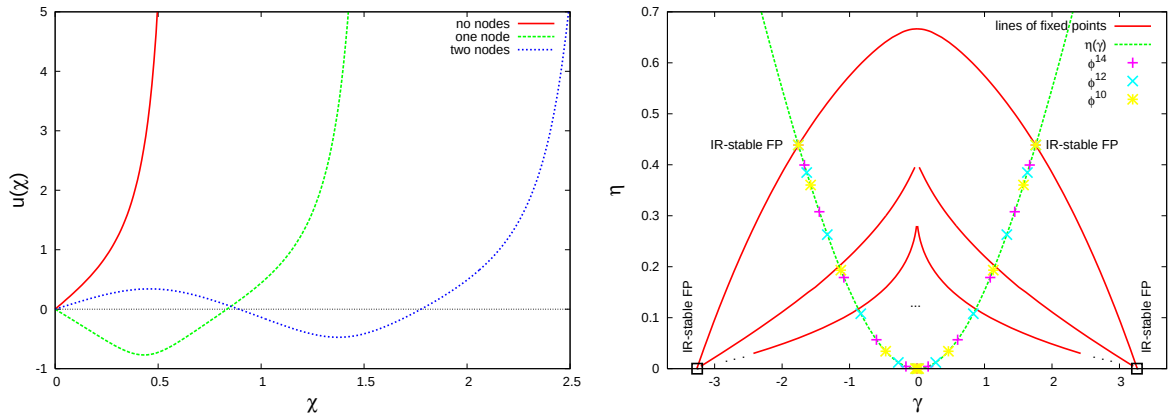

FIG. 7: Left panel: regular potentials for $\eta = 0.1$. Their asymptotic behavior is $\mathfrak{w}''(\chi) \sim \chi^{18}$; Right panel: Lines of fixed points in the η-γ plane (solid curves) and the anomalous dimension as a function of $\gamma = 2\lambda$ obtained from Eq. (54) (dotted curve). We also display the fixed point solutions obtained from a polynomial approximation of Eq. (52) and (53) for different truncations.

# nodes	η	ν_W
0	0.4386	1.2809
1	0.20	1.11
2	0.12	1.06

TABLE V: Critical exponents of the first fixed points.

ϕ_0. The potentials are therefore regular if the right-hand side of Eq. (60) vanishes for the same value ϕ_0, which is achieved by a fine-tuning of γ. The outermost curve in Fig. 7 (right panel) corresponds to a potential $\mathfrak{w}''_*$ with no nodes, the next curve to potentials with one node and the third curve to potentials with two nodes. We expect to find more curves for small η and γ corresponding to potentials with more nodes. In Fig. 7 (right panel) we also display $\eta(\gamma) = 4\gamma^2/(\gamma^2+8\pi)$ obtained from equation (53).

The polynomial approximation to the fixed point solution of Eq. (52) and Eq. (53) converges to the maximally IR-stable fixed point with $\eta = 0.4386$ and $\gamma = 1.759$, which is just the point of intersection with the line of fixed points corresponding to potentials with no nodes. The intersection points of the $\eta(\gamma)$ line with the other lines of fixed points with higher numbers of nodes then give estimates for the critical exponents of these other fixed points at next-to-leading order in the derivative expansion. E.g., we find $\eta \simeq 0.20$ for the fixed point with one node and $\eta \simeq 0.12$ for the fixed point with two nodes. The corresponding critical exponent ν_W then follows directly from the superscaling relation (57). They are listed in Tab. V. The point characterized by $\eta = 0$ and $\gamma = 3.529$ in Fig. 7 (right panel) (see appendix B) belongs to a solution of the type discussed in section VI, where the maximally IR-stable solution can be extended without cusps beyond the critical value of the potential $\mathfrak{w}''$.

D. Synthesis: derivative expansion results at leading order and next-to-leading order

At a first glance, the fixed-point potentials obtained at the various orders in the derivative expansion seem even qualitatively different. At leading-order, we find oscillating solutions, solutions with cusps, and solutions with a compact target space. By contrast, the next-to-leading-order solutions admit superpotentials that can be extended to infinite field amplitude with a standard powerlaw asymptotics $W'(\phi \to \infty) \sim \phi^{2/\eta-1} \to \infty$.

Of course, there are also many similarities, as the next-to-leading-order fixed-point potentials can be classified by their number of nodes, i.e., they typically exhibit an oscillating behavior for small fields. In addition, we expect the occurrence of superpotentials with singular structures at finite field values which have not been searched for as systematically as in the leading-order case.

The key to a unified understanding of both orders is provided by the anomalous dimension η, as the new large field asymptotics at next-to-leading order is induced by a nonzero value for η. It should be kept in mind that we deduce the nonzero value for η from a small-field expansion of the full flow of the wave function renormalization $Z_k(\phi)$. Beyond this expansion, the anomalous dimension will acquire a field dependence $\eta \to \eta(\phi)$. From the general form of the flow equation, we expect that the large-field limit is characterized by $\eta(\phi \to \infty) \to 0$. We therefore conjecture that the true large-field asymptotics of the fixed-point superpotentials lies in-between the leading- and next-to-leading-order results. More precisely, we expect that a standard asymptotic behavior $W'(\phi \to \infty) \to \infty$ persists, but the powerlaw behavior $\phi^{2/\eta-1}$ may be replaced by a stronger divergence.

In any case, the rapid convergence of the polynomial expansion in both orders of the derivative expansion, as well as quantitative agreement between observables derived from the polynomial expansion and from the full solution support the reliability of the overall picture arising from the derivative expansion.

VII. THE GAUSSIAN WESS-ZUMINO MODEL

In principle, each of the fixed points defines a different UV completion of the Wess-Zumino model and therefore a different physical system with a different number of physical parameters. In the following, we concentrate on the Wess-Zumino model defined at the Gaußian fixed point corresponding to an asymptotically free theory. At least seemingly, this is a natural choice, as it has also often been used in lattice computations. However, the Gaußian fixed point actually has infinitely many relevant directions, as is already revealed by perturbative power-counting. As a consequence, there are strictly speaking infinitely many physical parameters.

In practice, one usually starts with a classical superpotential including quadratic perturbations of the Gaußian fixed point, $W'_\Lambda = \bar\lambda_\Lambda(\phi^2 - \bar a_\Lambda^2)$, at the UV cutoff $k = \Lambda$, implying that infinitely many couplings have been set to zero at that scale. Since the RG trajectories are not regulator independent, it will still be difficult to compare our results with those of, say, lattice computations, as the same physical system with lattice regularization might have a very different action at the lattice cutoff $\Lambda = \pi/a$. In fact, we find a substantial quantitative regulator dependence for non-universal quantities within the functional RG calculations; see App. B which might imply that a meaningful comparison with other methods should only be made on a qualitative level.

On the other hand, one may interpret the choice of the regulator as belonging to the definition of the theory itself: the regulator together with the initial condition in the form of a quadratic perturbation specifies the RG trajectory uniquely also at a finite scale Λ. In the general case, this viewpoint has the disadvantage that a change of the cutoff scale Λ on the line of constant physics generically involves an adjustment of the couplings of infinitely many operators. In order to find out how much these operators actually affect the flow of the superpotential, we have varied the cutoff scale Λ. For a given Λ, we adjust the couplings in $W'_\Lambda = \bar\lambda_\Lambda(\phi^2 - \bar a_\Lambda^2)$ such that we obtain fixed reference couplings a_{Λ_0} and λ_{Λ_0} at a reference scale Λ_0, ignoring higher-order couplings. This way of looking at the cutoff-dependence is very much motivated by similar procedures in recent lattice simulations of the two-dimensional Wess-Zumino model in [4, 38]. For large enough Λ, the solutions of the flow equation show that the dependence of, e.g., the ground state energy at $k = 0$ on the actual cutoff scale is small. This observation helps making the viewpoint of including the regulator in the definition of the theory practicably applicable. Still, it has to be emphasized that we observe a significant regulator dependence of the nonuniversal quantities, see App. B.

A. Numerical solution of the flow equation in local-potential approximation

At the cutoff scale Λ, we start with $W'_\Lambda = \bar\lambda_\Lambda(\phi^2 - \bar a_\Lambda^2)$, where $\bar\lambda_\Lambda\phi^2$ is a relevant perturbation of the Gaußian fixed point. For large values of the field, the right-hand side of Eq. (38) vanishes such that $\partial_k W'_k \simeq 0$ and the effective potential remains close to the classical potential. It follows that the dimensionless potential $w_t = W_k/k$ diverges for large ϕ in the infrared. On the other hand, we expect that the dimensionful $W''(\phi) = k u_t(\phi)$ converges to zero for small fields, since u_t can be attracted by the maximally IR-stable fixed point and converges to a bounded function u.

Because of the singularity in the fixed point equation for u, the solution of the partial differential equation (38) poses a numerical challenge. To meet this challenge, we exploit the fact that the polynomial solutions with scale-dependent coefficients (40) yield excellent approximations to the solution of the full partial differential equation for small fields $\phi < \phi_{\rm crit}$. For the fixed-point solution, this has been demonstrated earlier, see Fig. 5, left panel. Thus, we use a polynomial approximation for $|\phi| < \phi_{\rm crit}$. For large fields $|\phi| > \phi_{\rm crit}$, the polynomial approximation fails and we solve the partial differential equation numerically. As boundary conditions for the numerical solutions, we impose $W'_k(\phi) = W'_\Lambda(\phi)$ for $|\phi| \to \infty$ and $W_k(\phi_{\rm crit})$ equal to the polynomial approximation at $\phi_{\rm crit}$ and scale k. Figure 8 (left panel) shows the flow of such a potential.

B. The phase diagram

Depending on the parameters in $W'_\Lambda = \bar\lambda_\Lambda(\phi^2 - \bar a_\Lambda^2)$ we may end up with a broken or unbroken supersymmetry in the infrared. Note that λ_k is dimensionful, whereas a_k is dimensionless. The rescaled dimensionless couplings have an index $t = \ln k/\Lambda$, e.g. $\lambda_k = k\lambda_t$ and $a_k = a_t$. In the following, we determine the parameter region for which supersymmetry is dynamically broken. A criterion for supersymmetry breaking is provided by a nonvanishing ground state energy, given by the minimal value of $V(\phi) = \frac{1}{2}W'^{\,2}(\phi)$, where $W' = W'_{k\to 0}$. The ground state energy is nonzero if and only if $W'(\phi) > 0$ for all ϕ. Since $W'(\phi)$ is minimal at the origin we may use the polynomial approximation for which $W'_k(0) = -\lambda_k \cdot a_k^2 = -(k\lambda_t)\cdot a_t^2$. The dimensionless coupling λ_t flows to the IR fixed-point value λ^*, whereas the coupling a_t^2 diverges for $k \to 0$ or equivalently for $t \to -\infty$, such that the dimensionful quantity $k\,\lambda_t \cdot a_t^2$ converges to a *finite value*. This is a direct consequence of the fact that the divergence of a_t^2 at the fixed point is governed by the critical exponent

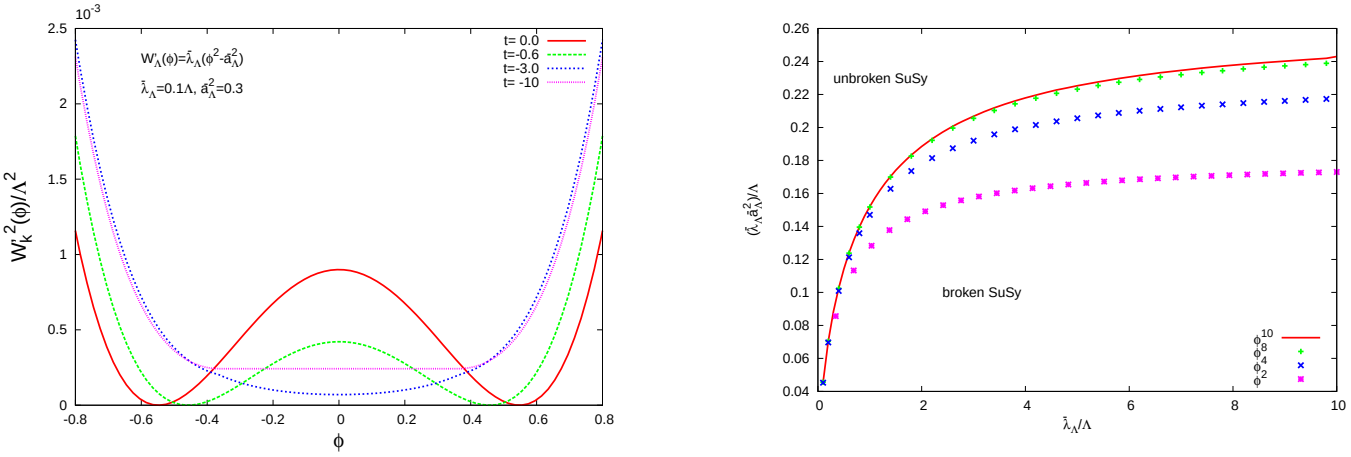

FIG. 8: Left panel: Flow of a potential with dynamical supersymmetry breaking, $W'_\Lambda(\phi) = \bar{\lambda}_\Lambda(\phi^2 - \bar{a}_\Lambda^2)$, $\Lambda = 1000$, $\bar{\lambda}_\Lambda = 100$, $\bar{a}_\Lambda^2 = 0.3$; Right panel: Phase diagram in the space of the dimensionless couplings specified at the cutoff scale Λ for different truncations.

$\theta^0 = 1$. The supersymmetric phase is characterized by $a_t^2 \to +\infty$ and a double well potential $W_k'^2$, whereas the broken phase is characterized by $a_t^2 \to -\infty$ and a single well potential.

This gives rise to a strong analogy between dynamical supersymmetry breaking in this and many other supersymmetric systems and quantum critical phenomena in strongly correlated fermion systems [18]: both phenomena are governed by a control parameter of the (super-)potential which plays the role of a bosonic mass term; see, e.g., [39] for an RG treatment of a semi-metal–superfluid quantum phase transition in a fermionic system. This control parameter, which is usually called δ in quantum critical phenomena, is associated to the combination $\delta = \bar{\lambda}_\Lambda \cdot \bar{a}_\Lambda^2/\Lambda$ in our case. The critical value $\delta_{\rm cr}$ of the control parameter marks a quantum critical point of a quantum phase transition.

In Fig. 8 (right panel), we depict the phase diagram in the space of dimensionful couplings $\bar{\lambda}_\Lambda$ and $\bar{\lambda}_\Lambda \cdot \bar{a}_\Lambda^2$ in units of the UV cutoff Λ for increasing truncation order.

In the ϕ^2 truncation, the system of differential equations reads (see equation (40))

$$\partial_t a_t^2 = \frac{1}{2\pi} - \frac{6\lambda_t^2 \cdot a_t^2}{\pi}, \quad \partial_t \lambda_t = -\lambda_t + \frac{6\lambda_t^3}{\pi}, \qquad (62)$$

which can be solved analytically. The phase transition curve in the $(\bar{\lambda}_\Lambda \bar{a}_\Lambda^2, \bar{\lambda})$ plane is given by the initial values for which $a^2_{t\to-\infty}$ changes sign. This condition yields

$$\frac{\bar{\lambda}_\Lambda \bar{a}_\Lambda^2}{\Lambda} = \frac{\arcsin(\alpha)}{\sqrt{24\pi}\,\alpha}, \qquad \alpha^2 = 1 - \frac{\pi\Lambda}{6\bar{\lambda}_\Lambda}. \qquad (63)$$

In order to find the approximate phase transition curve for the higher order polynomial truncations, we have integrated the corresponding systems of flow equations numerically. From the ϕ^2 to the ϕ^4 truncation, the transition curve moves considerably upwards because the coupling $b_{4,t}$ enters the flow equation for a_t^2 in Eq. (40). The higher couplings $b_{6,t}, b_{8,t}, \ldots$ enter the differential equation for a_t only indirectly, and, as a result, the approximate phase transition curves converge rapidly with increasing order of the truncation. We find that there exists a critical value for the cutoff parameter $\bar{\lambda}_\Lambda \bar{a}_\Lambda^2|_{\rm crit}$ characterizing the phase transition in the strong coupling limit $\bar{\lambda}_\Lambda \to \infty$. To lowest order, Eq. (63) leads to a critical value of $\bar{\lambda}_\Lambda \bar{a}_\Lambda^2|_{\rm crit}/\Lambda = \sqrt{\pi/96} \simeq 0.181$. Our best estimate for this critical value derived from a numerical higher-order solution is $\bar{\lambda}_\Lambda \bar{a}_\Lambda^2|_{\rm crit}/\Lambda \simeq 0.263$. We conclude that supersymmetry can never be broken dynamically above this critical value. This agrees qualitatively with earlier results in the literature [22, 25].

A more quantitative comparison to lattice simulation is inflicted by the strong regulator dependence of nonuniversal quantities, such as the bare critical coupling values discussed above, see also App. B. For instance in [24, 25], the phase diagram and the ground state energy of the present model were investigated anew. For a fixed $\bar{\lambda}_\Lambda/\Lambda = 0.5$, a phase transition from a state with broken to a state with unbroken supersymmetry was observed at the critical value $(\bar{\lambda}\bar{a}^2)|_{\rm crit}/\Lambda = 0.48$. With two different methods they obtained 0.40 and 0.52 for this critical value but they state 0.48 to be the most solid value. In these works, the thermodynamic limit has been performed without an accompanying continuum extrapolation. On the other hand, the quoted numbers for $(\bar{\lambda}\bar{a}^2)_\Lambda$ were in reasonable good agreement with earlier results obtained with the help of the worldline path integral method [28]. As demonstrated in App. B, a direct comparison of bare quantities between the present work and [24, 25] is anyway not meaningful due to the scheme dependence. If more lattice points in the phase diagram were available, dimensionless coupling ratios could be compared which are likely to be less affected by scheme dependencies.

C. Mass scaling

The scale-dependent bosonic mass can be read off from the bosonic potential in the on-shell formulation, which is given by $\bar{V}_k(\phi) = \frac{1}{2}(W_k'(\phi))^2$ in our truncation. In terms of renormalized fields $\chi = Z_k\phi$, the dimensionful renormalized bosonic potential and bosonic mass thus is

$$V_k(\chi) = \frac{1}{2}\,\frac{1}{Z_k^2}\left(W_k'(\chi/Z_k)\right)^2, \quad m_k^2 = V_k''(\chi_{\min}), \quad (64)$$

where $\chi_{\min}$ denotes the minimum of the effective potential $V_k(\chi)$. The true mass can then be read off in the limit $m = \lim_{k\to 0} m_k$.

In the broken phase, the minimum of both V_k and W_k' is at $\chi = 0$, such that the bosonic mass yields

$$m_k^2 = \frac{1}{Z_k^4}\,W_k'(0)W_k'''(0) = 2k^2\,\lambda_t^2|a_t^2|, \quad (65)$$

where we have used the fact that the renormalized parameter a_t^2 is negative. Assuming that the system is dominated by the maximally IR-stable fixed point with $\lambda_t \to \lambda^*$ and $a_t^2 \sim k^{-1/\nu_W}$, the renormalized mass scales as

$$m_k^2 \sim k^{1+\frac{\eta}{2}} \quad (66)$$

where we have employed the superscaling relation (57). For $\eta > -2$, the renormalized bosonic mass scales to zero upon attraction of the maximally IR-stable fixed point. Indeed, for the Gaußian Wess-Zumino model considered here, we observe that the flow in the broken phase is always attracted by the maximally IR-stable fixed point. Together with the fact that the broken phase also goes along with a massless goldstino, we conclude that the broken phase remains massless in both degrees of freedom.

In a certain sense, the underlying limit $k \to 0$ represents an extreme point of view. Any experiment as well as any lattice simulation will involve an IR cutoff scale $k_{\rm m}$ characterizing the measurement, e.g., the scale of a momentum transfer, the detector size or the lattice volume. Any measurement therefore is not sensitive to $k \to 0$ but to $k \to k_{\rm m} > 0$. We conclude that any measurement of the bosonic mass in the broken phase will give a nonzero answer proportional to the measurement scale, whereas the goldstino will be truly massless.

In the broken phase, the superscaling relation also has a special consequence for the unrenormalized potential. We observe that

$$W'(0) = -\bar{\lambda}_k\bar{a}_k^2 = -kZ_k\lambda_t a_t^2 \sim k^{1-\frac{\eta}{2}}\,k^{-1/\nu_W} \to \text{const.}, \quad (67)$$

where we have used Eq. (57) and $Z_k \sim k^{-\eta/2}$. Therefore, the flow of the superpotential freezes out near the origin if the system is in the domain of attraction of the maximally IR-stable fixed point.

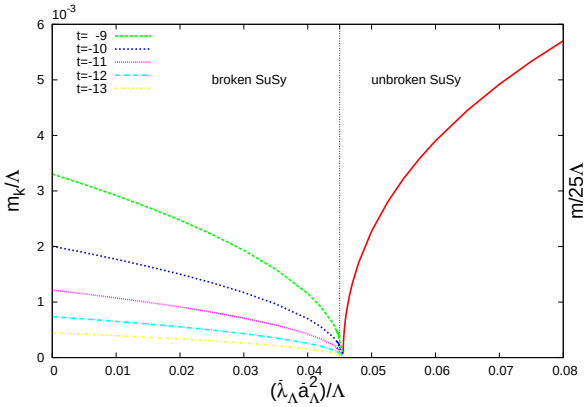

FIG. 9: Renormalized mass at different scales k as a function of the initial condition $\bar{\lambda}_\Lambda\bar{a}_\Lambda^2$ at an initial coupling of $\bar{\lambda}_\Lambda = 0.1$.

In the supersymmetric phase, the bosonic as well as the fermionic mass is given by

$$m_k^2 = \frac{1}{Z_k^4}\left(W_k''(\chi_{\min}/Z_k)\right)^2, \quad (68)$$

where we made use of the fact that W_k' vanishes at the minimum. For typical flows, W_k'' remains positive at the minimum also in the $k \to 0$ limit. This leads to a generic decoupling of the massive modes, once k drops below the mass threshold. For an accurate inclusion of this mass decoupling, also the anomalous dimension needs to be evaluated at the minimum $\chi_{\min}$, implying $\eta \to 0$ for $k^2 \ll m_k^2$, cf. Eq. (53).

For simplicity, we confine ourselves to the local-potential approximation and set $Z_k \to 1$, $\eta \to 0$ for a computation of the masses across the phase transition. Our results are displayed in Fig. 9 as a function of the initial-condition parameter $\bar{\lambda}_\Lambda\bar{a}_\Lambda^2$ of the relevant direction. The calculation has been performed at an initial value for the coupling of $\bar{\lambda}_\Lambda/\Lambda = 0.1$. We observe a critical value of $\bar{\lambda}_\Lambda\bar{a}_\Lambda^2|_{\rm crit}/\Lambda \simeq 0.045$, above which supersymmetry remains unbroken and the theory is massive. Both masses vanish at the quantum phase transition. Below the critical value, supersymmetry is broken and the goldstino is massless. The bosonic mass also approaches zero for $k \to 0$, but remains finite for any finite value of k, potentially representing a measurement scale.

VIII. CONCLUSIONS

In this work, we have constructed a manifestly supersymmetric flow equation for the application of the functional RG to the two dimensional $\mathcal{N} = 1$ Wess-Zumino model. The regularization turns out to be similar to the one in supersymmetric quantum mechanics. This is not surprising since supersymmetric quantum mechanics can be derived from the Wess-Zumino model by a dimensional reduction.

For approximate solutions to the flow equation, we have employed an expansion of the effective action in terms of field operators containing increasing powers of supercovariant derivatives. This provides a systematic approximation scheme that preserves supersymmetry. We obtain a flow equation for the superpotential and, at next-to-leading order, for the wave function renormalization.

The Wess-Zumino model has a highly nontrivial fixed-point structure in terms of scaling solutions for the superpotential. At leading- as well as next-to-leading order in the derivative expansion, we find fixed-point superpotentials which can be classified by an increasing number of relevant directions. At leading order, the classification of fixed-point solutions can largely be done on analytical grounds. Here, we find oscillating sine-Gordon-type or even bouncing solutions on the one hand, and solutions confining the field to a compact target space on the other hand. For the regular oscillating solutions, the large-field asymptotics is turned into a standard form $W'(\phi \to \infty) \to \infty$ at next-to-leading order, where the fixed-point superpotentials can be classified also according to their number of nodes. This is reminiscent to fixed points of the effective potential in two-dimensional bosonic theories which can be related to conformal field theories [34, 35]. Exploring the connection between the present supersymmetric models at their fixed points and conformal field theories remains an interesting question for future work.

Each fixed point defines its own universality class, the physics of which is determined by the RG relevant directions of the fixed points. In other words, each fixed point defines a different Wess-Zumino model with the number of physical parameters given by the number of relevant directions. One extreme is provided by the Gaußian fixed point which has infinitely many relevant directions in agreement with perturbative power-counting arguments. The other extreme is given by the maximally IR-stable fixed point which has only one relevant direction. We have demonstrated that this relevant direction is exactly given by a_t^2 and is shared by all other fixed points as well.

At leading- and next-to-leading order, the critical exponent associated with this relevant a_t^2 direction can be computed exactly. At next-to-leading order, this yields an intriguing relation between this critical exponent of the superpotential $\nu_W = 1/\theta^0$ and the anomalous dimension η of the field. As such a relation between critical exponents associated with correlation functions is not known from Ising-type systems (where thermodynamical exponents are related by scaling relations among each other and by hyperscaling relations to the correlation exponents), this *superscaling* relation appears to be a unique property of supersymmetric theories.

The superscaling relation has a direct consequence for the renormalized superpotential W at the origin in field space. It dictates a freeze out of the derivative of the superpotential at the origin in the deep IR, if the system is governed by one of the fixed points.

As an example for a model with dynamical supersymmetry breaking, we considered the Wess-Zumino model defined by a quadratic perturbation of the Gaußian fixed point. In addition to the initial coupling value $\lambda|_\Lambda$, the model has a control parameter $\lambda a^2|_\Lambda$ the value of which decides about the realization of supersymmetry by the ground state of the theory. At a given coupling, supersymmetry can only be broken for $\lambda a^2|_\Lambda$ below a certain critical value which is in accord with a general argument by Witten. We have computed the critical line of quantum phase transitions in the coupling–control-parameter plane for a wide range from weak to strong coupling. Most importantly, the control parameter stays finite even at arbitrarily large coupling.

We have also computed the masses of the lowest fermionic and bosonic excitations across the quantum phase transition. In the supersymmetric phase, both masses are equal and nonzero, but drop to zero at the phase transition. In the broken phase, the fermion has a massless goldstino mode. We observe that the boson also becomes massless in the broken phase in the deep IR, $k \to 0$, but stays finite for any finite k. Associating k with a typical measurement momentum scale (say, inverse length of a detector), our results predict that the bosonic mass in the broken phase is proportional to the momentum scale set by the detector.

The critical properties of the quantum phase transition remain an interesting open problem. In this work, we have considered the ground state energy or the bosonic and fermionic masses of the theory as order parameters for the symmetry. In our numerical results, we have found no hint for typical scaling behavior of these quantities near the phase transition so far. Actually, a true field-valued order parameter is given in terms of the expectation value of the auxiliary field F. It is therefore natural to expect that order-parameter fluctuations of the F field play an important role near criticality and eventually establish a scaling behavior. Technically, this requires the inclusion of potential terms for the F field. As these appear at higher orders in the supercovariant derivative expansion, a quantitative description of the critical regime remains a technical challenge.

From the perspective of the functional-RG tool box, we have solved the flow equation for the superpotential both in a polynomial expansion as well as with a full numerical solution of the corresponding partial differential equation. Whereas the polynomial approximation for the potential is only reliable in the vicinity of its expansion point with a finite radius of convergence, it often suffices to extract reliable quantitative information about physical observables such as critical exponents or the phase diagram.

In the context of the phase diagram of the Gaußian Wess-Zumino model, we have expressed our concern that a quantitative comparison with other methods such as lattice simulations can be plagued by the fact that the model has infinitely many relevant directions. As a direct consequence, the results of the model defined by a

certain (say quadratic) perturbation of the fixed point at a fixed UV scale Λ are regulator dependent, as this defining initial condition is not universal. A much better comparison could arise from defining a Wess-Zumino model, e.g., in the vicinity of the next-to-maximally IR-stable fixed point, where there are only two relevant directions and thus two tunable physical parameters. Fixing these parameters in terms of two observables, all other quantities are a universal scheme-independent prediction of the theory.

Acknowledgments

Helpful discussions with G. Bergner, C. Wozar, T. Fischbacher and T. Kaestner are gratefully acknowledged. FS acknowledges support by the Studienstiftung des deutschen Volkes. This work has been supported by the DFG-Research Training Group "Quantum-and Gravitational Fields" GRK 1523/1, the DFG grants Wi 777/10-1 and Gi 328/5-1 (Heisenberg program).

Appendix A: Flow equation with wave function renormalization

At next-to-leading order in the derivative expansion, a field-independent wave function renormalization is included in the truncation via

$$\Gamma_k[\phi,F,\bar\psi,\psi]=\int d^2x\left[Z_k^2\left(\tfrac{1}{2}\partial_\mu\phi\partial^\mu\phi+\tfrac{i}{2}\bar\psi\partial\!\!\!/\psi-\tfrac{1}{2}F^2\right)+\tfrac{1}{2}W_k''(\phi)\bar\psi\gamma_*\psi-W_k'(\phi)F\right]. \quad \text{(A1)}$$

The cutoff action reads

$$\Delta S_k=\frac{1}{2}\int(\phi,F)Z_k^2R_k^{\rm B}\begin{pmatrix}\phi\\F\end{pmatrix}+\frac{1}{2}\int dx^2\bar\psi Z_k^2R_k^{\rm F}\psi, \quad \text{(A2)}$$

with $R_k^{\rm B}$ and $R_k^{\rm F}$ given in Eq. (28). The flow equation for the superpotential is obtained by a projection onto the terms linear in the auxiliary field and by integration with respect to ϕ. We obtain a similar flow equation as in Eq. (36),

$$\begin{aligned}\partial_kW_k(\phi)=&\frac{1}{2}\int\frac{d^2p}{4\pi^2}\frac{(1+r_2)Z_k^2\,\partial_k(r_1Z_k^2)}{\Delta}\\&-\frac{1}{2}\int\frac{d^2p}{4\pi^2}\frac{(W_k''(\phi)+r_1Z_k^2)\partial_k(r_2Z_k^2)}{\Delta}.\end{aligned} \quad \text{(A3)}$$

Including the wave function renormalization, the expression in the denominator reads

$$\Delta=Z_k^4\,p^2(1+r_2)^2+(W_k''+r_1Z_k^2)^2. \quad \text{(A4)}$$

For the flow of the wave function renormalization, we project the flow equation onto the terms quadratic in the auxiliary field. As we consider only a field-independent wave function renormalization, we can also project onto $\phi=0$

$$\begin{aligned}\partial_kZ^2=&-W_k'''(\phi)^2Z_k^2\int\frac{d^2p}{4\pi^2}\,(1+r_2)\times\\&\left[\frac{2Z_k^2\left(W_k''(\phi)+r_1Z_k^2\right)(1+r_2)}{\Delta^3}\,\partial_k(r_1Z_k^2)\right.\\&\left.+\frac{Z_k^4p^2(1+r_2)^2-\left(W_k''(\phi)+r_1Z_k^2\right)^2}{\Delta^3}\,\partial_k(r_2Z_k^2)\right]_{\phi=0}.\end{aligned} \quad \text{(A5)}$$

As regulator shape functions, we choose $r_1=0$ and $r_2=(k^2/p^2-1)\theta(1-p^2/k^2)$ for which the momentum integrals in the flow equations can be calculated analytically. We obtain

$$\begin{aligned}\partial_kW_k=&-\frac{W_k''^2\partial_k(k^2Z_k^2)+k^4Z_k^4\partial_kZ_k^2}{8\pi W_k''^3}\ln\left(1+\frac{W_k''^2}{k^2Z_k^4}\right),\\&+\frac{k^2\partial_kZ_k^2}{8\pi W_k''}\end{aligned} \quad \text{(A6)}$$

$$\begin{aligned}\partial_kZ_k^2=&\frac{k}{4\pi}\left(\frac{Z_kW_k'''}{W_k''^2}\right)^2\left[\frac{W_k''^2k\partial_kZ_k^2}{W_k''^2+k^2Z_k^4}\right.\\&\left.-k\partial_kZ_k^2\ln\left(1+\frac{W_k''^2}{k^2Z_k^4}\right)-\frac{2W_k''^4Z_k^2}{(W_k''^2+k^2Z_k^4)^2}\right]_{\phi=0}.\end{aligned} \quad \text{(A7)}$$

For the renormalized fields, $\chi=Z_k\phi$, the superpotential scales as $\mathscr{W}_k(\chi)=W_k(\phi)$ and $\mathscr{W}_k'=W_k'/Z_k$, $\mathscr{W}_k''=W_k''/Z_k^2$, ... In terms of the anomalous dimension $\eta=-\partial_tZ_k^2/Z_k^2$, the preceding flow equations read

$$\begin{aligned}k\partial_k\mathscr{W}_k(\chi)=&\frac{\eta}{2}\chi\mathscr{W}_k'-\frac{\eta\,k^2}{8\pi\mathscr{W}_k''}\\&+\frac{(\eta-2)k^2\mathscr{W}_k''^2+\eta k^4}{8\pi\mathscr{W}_k''^3}\ln\left(1+\frac{\mathscr{W}_k''^2}{k^2}\right),\end{aligned} \quad \text{(A8)}$$

$$\begin{aligned}\eta=&\frac{k^2}{4\pi}\left(\frac{\mathscr{W}_k'''}{\mathscr{W}_k''^2}\right)^2\left[\frac{\eta\mathscr{W}_k''^2}{\mathscr{W}_k''^2+k^2}\right.\\&\left.-\eta\ln\left(1+\frac{\mathscr{W}_k''^2}{k^2}\right)+\frac{2\mathscr{W}_k''^4}{(\mathscr{W}_k''^2+k^2)^2}\right]_{\phi=0}.\end{aligned} \quad \text{(A9)}$$

In terms of the dimensionless superpotential $\mathfrak{w}(\chi)=\mathscr{W}(\chi)/k$, this reads

$$\begin{aligned}\partial_t\mathfrak{w}_k(\chi)=&\frac{\eta}{2}\chi\mathfrak{w}_k'-\mathfrak{w}_k-\frac{\eta}{8\pi\mathfrak{w}_k''}\\&+\frac{(\eta-2)\mathfrak{w}_k''^2+\eta}{8\pi\mathfrak{w}_k''^3}\ln\left(1+\mathfrak{w}_k''^2\right),\end{aligned} \quad \text{(A10)}$$

$$\begin{aligned}\eta=&\frac{1}{4\pi}\left(\frac{\mathfrak{w}_k'''}{\mathfrak{w}_k''^2}\right)^2\left[\frac{\eta\mathfrak{w}_k''^2}{\mathfrak{w}_k''^2+1}\right.\\&\left.-\eta\ln\left(1+\mathfrak{w}_k''^2\right)+\frac{2\mathfrak{w}_k''^4}{(\mathfrak{w}_k''^2+1)^2}\right]_{\phi=0},\end{aligned} \quad \text{(A11)}$$

which agrees with Eqs. (52) and (53).

1. Polynomial approximation

Next, we perform a polynomial expansion of the superpotential flow Eq. (A10) including wave function renormalization. We use the conventions $\mathfrak{w}_t'(\chi) = \lambda_t(\chi^2 - a_t^2) + \sum_{n=1}^{N} b_{2n,t}\chi^{2n}$, leading to the following system of coupled equations:

$$\begin{aligned}
\eta_t =& \frac{(4-\eta_t)\lambda_t^2}{2\pi} \qquad\qquad (A12)\\
\partial_t a_t^2 =& \frac{1}{8\pi}(4-\eta_t) - \eta_t a_t^2 \\
&- \frac{a_t^2}{\lambda_t}\left(\frac{3\left(\lambda_t^3 - b_{4,t}\right)}{\pi} - \frac{\left(2\lambda_t^3 - 3b_{4,t}\right)\eta_t}{4\pi}\right)\\
\partial_t \lambda_t =& -\lambda_t + \frac{3\left(\lambda_t^3 - b_{4,t}\right)}{\pi} - \frac{\left(2\lambda_t^3 - 3b_{4,t}\right)\eta_t}{4\pi} + \frac{3}{2}\eta_t\lambda_t\\
\partial_t b_{4,t} =& -b_{4,t} - \frac{5(8-\eta_t)\lambda_t^5 - 15b_{4,t}(6-\eta_t)\lambda_t^2}{3\pi} \qquad (A13)\\
&- \frac{45b_{6,t}(4-\eta_t)}{24\pi} + \frac{5}{2}\eta_t b_{4,t}\\
\partial_t b_{6,t} =& -b_{6,t} - \frac{7b_{8,t}(4-\eta_t)}{2\pi} - \frac{70b_{4,t}(8-\eta_t)\lambda_t^4}{3\pi}\\
&+ \frac{28(10-\eta_t)\lambda_t^7}{5\pi} + \frac{7(3b_{6,t}\lambda_t^2 + 4b_{4,t}^2\lambda_t)(6-\eta_t)}{2\pi}\\
&+ \frac{7}{2}\eta_t b_{6,t}\\
&\vdots
\end{aligned}$$

Again, the first-order coupling a_t does not influence the higher-order flows. Setting the left-hand side to zero, we find a nonlinear system of algebraic equations for the fixed-point couplings. The solutions determine the coefficients of the fixed-point superpotential in the polynomial expansion.

For a truncation at $2n$th order, we again find $2n+1$ real fixed points. As proved in the main text, each fixed point has at least one relevant direction which is provided by the a_t^2 direction. The maximally IR-stable fixed point has only this relevant (IR-unstable) direction. The other fixed points can be classified according to their increasing number of further relevant directions. The Gaußian fixed point remains fully UV attractive also at this order of the derivative expansion.

	coefficients at IR-fixed point						
$2n$	λ^*	b_4^*	b_6^*	b_8^*	b_{10}^*	b_{12}^*	b_{14}^*
2	1.023						
4	1.405	1.301					
6	1.540	2.040	3.097				
8	1.593	2.374	4.868	8.651			
10	1.615	2.523	5.725	13.38	26.00		
12	1.625	2.590	6.124	15.70	39.55	81.19	
14	1.629	2.620	6.308	16.79	46.11	121.8	259.4

TABLE VI: Coefficients of the first few couplings in a polynomial expansion of the fixed-point superpotential at the maximally IR stable fixed-point for different truncations. The expected nonuniversal deviations from Tab. I are due to the use of a different regulator.

Appendix B: Regulator dependence

In this appendix, we repeat several studies of the local-potential approximation as done in the main text but now for a different regulator shape function $r_2 = (k^2/p^2 - 1)\theta(p^2/k^2 - 1)$. This is actually equivalent to the regulator used for at next-to-leading order in the main text. On the one hand, this regulator comparison gives a rough estimate of how nonuniversal quantities may vary. On the other hand, it supports all structural results of the main text, which should in any case be universal.

The flow equation for the superpotential (36) now takes the form

$$\partial_k W_k(\phi) = \frac{k}{4\pi W_k''(\phi)} \ln\left(\frac{k^2}{k^2 + W_k''(\phi)^2}\right). \qquad (B1)$$

In terms of the dimensionless quantity $kw_t = W_k$, this reads

$$\partial_t w_t(\phi) + w_t(\phi) = -\frac{\ln\left(1 + w_t''(\phi)^2\right)}{4\pi w_t''(\phi)}. \qquad (B2)$$

This equation is regular at $w'' = 0$ since $\ln(1+x) = x - \frac{x^2}{2} + \frac{x^3}{3} \mp \ldots$ for small x. The second derivative of this equation at the fixed point $\partial_t w_* = 0$ is given by ($u = w_*''$)

$$\begin{aligned}
u'' =& \frac{4\pi u^3\left(u^2+1\right)}{(u^2+1)\ln(u^2+1) - 2u^2} \qquad (B3)\\
&+ \frac{2u\left(u^2-1\right)u'^2}{(u^2+1)\left(2u^2 - \ln(u^2+1)(u^2+1)\right)} + \frac{2u'^2}{u},
\end{aligned}$$

which agrees with Eq. (60) in the limit $\eta = 0$. It has the same singularity structure as the corresponding Eq. (48) for the simpler regulator used in the main text. The fourth derivative becomes singular if

$$u^2 = \frac{1}{2}(u^2+1)\ln(u^2+1) \quad \Rightarrow \quad u \simeq 1.9803, \qquad (B4)$$

(to be compared with the singular point $u = 1$ for the simpler regulator). Overall, we find the same types of solutions as discussed in section VI. In particular, we again find oscillatory solutions and a maximally IR-stable fixed point with one relevant direction.

A polynomial expansion of Eq. (B3) with $u = 2\lambda_t^2\phi + \sum_{n=2}^{N} 2n \cdot b_{2n,t}\phi^{2n-1}$ yields a system of algebraic equations that determine the expansion coefficients of the fixed-point potential. This system is given by Eq. (A13)

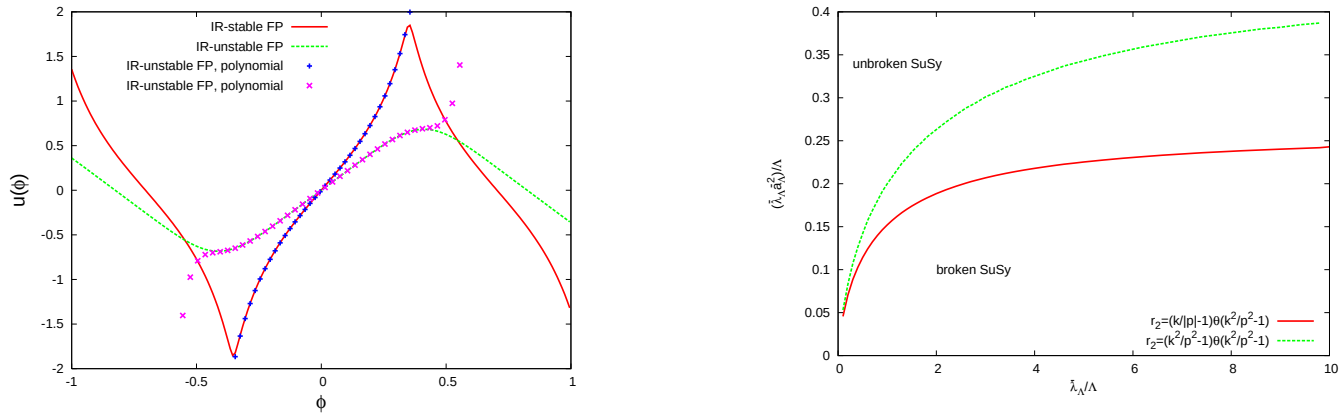

FIG. 10: *Left panel:* fixed-point superpotentials calculated from Eq. (B3) with $\lambda = 1.6295$ for the maximally IR-stable fixed-point and $\lambda = 1.0411$ for an IR-unstable fixed-point. *Right panel:* Comparison between the critical bare values for $(\lambda a^2)_{t=0}$ characterizing the phase transition calculated with the regulators $r_2 = (k/p-1)\theta(p^2/k^2-1)$ and $r_2 = (k^2/p^2-1)\theta(p^2/k^2-1)$. The difference is attributed to a strong scheme dependence of this nonuniversal quantity.

λ^*	Critical exponents θ^I							
± 1.6315	-1.31	-7.10	-19.3	-42.7	-84.8	-158	-285	-522
± 1.4399	5.43	-1.49	-10.1	-28.2	-61.8	-122	-227	-426
± 1.1463	19.5	4.07	-1.51	-11.8	-33.9	-75.7	-152	-298
$\pm .81753$	28.1	12.4	3.23	-1.39	-12.5	-37.3	-85.7	-182
$\pm .49584$	$20.4 + 3.09i$	$20.4 - 3.09i$	8.06	2.54	-1.16	-12.5	-38.9	-95.0
$\pm .22322$	$11.9 + 8.85i$	$11.9 - 8.85i$	8.69	5.07	1.96	-0.859	-12.0	-39.8
$\pm .04903$	$4.27 + 1.14i$	$4.27 - 1.14i$	$2.91 + 6.63i$	$2.91 - 6.63i$	2.84	1.47	-0.547	-11.1
± 0.00042	$1.57 + 0.125i$	$1.57 - 0.125i$	$1.43 + 0.70i$	$1.43 - 0.703i$	1.14	$0.542 + 0.982i$	$0.542 - 0.982i$	-0.222
0	1	1	1	1	1	1	1	1

TABLE VII: Critical exponents θ^I (negative eigenvalues of the stability matrix) for a polynomial truncation at $2n = 16$ for the nine different fix points in the local-potential approximation. The first exponent $\theta^0 = 1$ which is common to all fixed points is not shown here. This table should be compared with Tab. II which has been computed with a different regulator. For all positive critical exponents, we find a remarkable degree of universality, as these exponents for the different regulators differ if at all by at most 10%. The subleading negative critical exponents show larger variations.

without the equation for a^2, with $\eta = 0$ and the derivatives with respect to t set equal to zero.

The results for the fixed-point couplings for the maximally IR-stable fixed-point are displayed in Tab. VI for different truncations. A comparison with Tab. I reveals the regulator-dependent variations of these nonuniversal quantities.

We find that the coupling λ_* converges quickly. Again, the polynomial expansion provides a good approximation to the solution of the partial differential equation for the first half period. This is displayed in Fig. 10, left panel.

By contrast, the universal critical exponents θ^I at the fixed points are much less regulator dependent. This is demonstrated in Tab. VII which should be read side by side with Tab. II for a different regulator. For all positive critical exponents, we find a remarkable degree of universality, as these exponents for the different regulators differ – if at all – by at most 10%. The subleading negative critical exponents show larger variations and thus require higher orders in the derivative expansion for a quantitatively reliable prediction.

We also calculate the phase diagram with this regulator for a truncation at $2n = 10$ and compare both regulators $r_2 = (k/|p| - 1)\theta(p^2/k^2 - 1)$ and $r_2 = (k^2/p^2 - 1)\theta(p^2/k^2 - 1)$ in Fig. 10, right panel. The nonuniversal values for λa at the phase transition differ roughly by a factor of two. This clearly demonstrates that a naive comparison of bare couplings is substantially inflicted by the regularization scheme.

[1] Simon Catterall, David B. Kaplan, and Mithat Unsal. Exact lattice supersymmetry. 2009, arXiv:0903.4881 [hep-lat].
[2] Joel Giedt. Deconstruction and other approaches to su-

persymmetric lattice field theories. *Int. J. Mod. Phys.*, A21:3039–3094, 2006, hep-lat/0602007.

[3] Georg Bergner, Tobias Kaestner, Sebastian Uhlmann, and Andreas Wipf. Low-dimensional supersymmetric lattice models. *Annals Phys.*, 323:946–988, 2008, arxiv:0705.2212 [hep-lat].

[4] Tobias Kaestner, Georg Bergner, Sebastian Uhlmann, Andreas Wipf, and Christian Wozar. Two-Dimensional Wess-Zumino Models at Intermediate Couplings. 2008, arXiv:0807.1905 [hep-lat].

[5] K. Aoki. Introduction to the nonperturbative renormalization group and its recent applications. *Int. J. Mod. Phys.*, B14:1249–1326, 2000.

[6] Jurgen Berges, Nikolaos Tetradis, and Christof Wetterich. Non-perturbative renormalization flow in quantum field theory and statistical physics. *Phys. Rept.*, 363:223–386, 2002. hep-ph/0005122.

[7] Daniel F. Litim and Jan M. Pawlowski. On gauge invariant Wilsonian flows. 1998. hep-th/9901063.

[8] Jan M. Pawlowski. Aspects of the functional renormalisation group. *Annals Phys.*, 322:2831–2915, 2007, hep-th/0512261.

[9] Holger Gies. Introduction to the functional RG and applications to gauge theories. 2006, hep-ph/0611146.

[10] Hidenori Sonoda. The Exact Renormalization Group – renormalization theory revisited –. 2007, arXiv:0710.1662 [hep-th].

[11] M. Bonini and F. Vian. Wilson renormalization group for supersymmetric gauge theories and gauge anomalies. *Nucl. Phys.*, B532:473–497, 1998, hep-th/9802196.

[12] F. Vian. Supersymmetric gauge theories in the exact renormalization group approach. 1998, hep-th/9811055.

[13] Sven Falkenberg and Bodo Geyer. Effective average action in N = 1 super-Yang-Mills theory. *Phys. Rev.*, D58:085004, 1998, hep-th/9802113.

[14] S. Arnone and K. Yoshida. Application of exact renormalization group techniques to the non-perturbative study of supersymmetric field theory. *Int. J. Mod. Phys.*, B18:469–478, 2004.

[15] Stefano Arnone, Francesco Guerrieri, and Kensuke Yoshida. N = 1* model and glueball superpotential from renormalization group improved perturbation theory. *JHEP*, 05:031, 2004, hep-th/0402035.

[16] Oliver J. Rosten. On the Renormalization of Theories of a Scalar Chiral Superfield. 2008, arXiv:0808.2150 [hep-th].

[17] Hidenori Sonoda and Kayhan Ulker. Construction of a Wilson action for the Wess-Zumino model. 2008, arXiv:0804.1072 [hep-th].

[18] Holger Gies, Franziska Synatschke, and Andreas Wipf. Supersymmetry breaking as a quantum phase transition. 2009, arXiv:0906.5492 [hep-th].

[19] Franziska Synatschke, Georg Bergner, Holger Gies, and Andreas Wipf. Flow Equation for Supersymmetric Quantum Mechanics. *JHEP*, 03:028, 2009. arXiv:0809.4396 [hep-th]

[20] Atsushi Horikoshi, Ken-Ichi Aoki, Masa-aki Taniguchi, and Haruhiko Terao. Non-perturbative renormalization group and quantum tunnelling. 1998, hep-th/9812050.

[21] M. Weyrauch. Functional renormalization group and quantum tunnelling. *J. Phys.*, A39:649–666, 2006.

[22] Edward Witten. Constraints on Supersymmetry Breaking. *Nucl. Phys.*, B202:253, 1982.

[23] J. Ranft and A. Schiller. Hamiltonian Monte Carlo study of (1+1)-dimensional models with restricted supersymmetry on the lattice. *Physics Letters B*, 138(1-3):166 – 170, 1984.

[24] Matteo Beccaria, Gian Fabrizio De Angelis, Massimo Campostrini, and Alessandra Feo. Phase diagram of the lattice Wess-Zumino model from rigorous lower bounds on the energy. *Phys. Rev.*, D70:035011, 2004.

[25] Matteo Beccaria, Massimo Campostrini, and Alessandra Feo. Supersymmetry breaking in two dimensions: The lattice N = 1 Wess-Zumino model. *Phys. Rev.*, D69:095010, 2004.

[26] Maarten F. L. Golterman and Donald N. Petcher. A local interactive lattice model with supersymmetry. *Nucl. Phys.*, B319:307–341, 1989.

[27] Simon Catterall and Sergey Karamov. A lattice study of the two-dimensional Wess Zumino model. *Phys. Rev.*, D68:014503, 2003.

[28] Matteo Beccaria and Carlo Rampino. World-line path integral study of supersymmetry breaking in the Wess-Zumino model. *Phys. Rev.*, D67:127701, 2003.

[29] Sidney R. Coleman and Erick J. Weinberg. Radiative Corrections as the Origin of Spontaneous Symmetry Breaking. *Phys. Rev.*, D7:1888–1910, 1973.

[30] T. Murphy and L. O'Raifeartaigh. A note on supersymmetry breaking in 1+1 dimensions. *Nucl. Phys.*, B218:484–492, 1983.

[31] Georg Bergner. *Symmetries and the methods of quantum field theory: Supersymmetry on a space-time lattice*. PhD Thesis (University Jena), 2009. unpublished.

[32] Jochen Bartels and J. B. Bronzan. Supersymmetry on a lattice. *Phys. Rev.*, D28:818, 1983.

[33] Christof Wetterich. Exact evolution equation for the effective potential. *Phys. Lett.*, B301:90–94, 1993.

[34] Rui Neves, Yuri Kubyshin, and Robertus Potting. Polchinski ERG equation and 2D scalar field theory. 1998, hep-th/9811151.

[35] Tim R. Morris. The Renormalization group and two-dimensional multicritical effective scalar field theory. *Phys. Lett.*, B345:139–148, 1995.

[36] Steven Weinberg. Critical Phenomena for Field Theorists. Lectures presented at Int. School of Subnuclear Physics, Ettore Majorana, Erice, Sicily, Jul 23 - Aug 8, 1976.

[37] A.B. Zamolodchikov. Conformal Symmetry and Multicritical Points in Two-Dimensional Quantum Field Theory. *Yad. Fiz.*, 44:529, 1986.

[38] Christian Wozar, Georg Bergner, Tobias Kaestner, Sebastian Uhlmann, and Andreas Wipf. Numerical Investigation of the 2D N=2 Wess-Zumino Model. 2008, arXiv:0809.2176 [hep-lat].

[39] P. Strack, S. Takei, and W. Metzner. Anomalous scaling of fermions and order parameter fluctuations at quantum criticality, 2009, arXiv:0905.3894 [cond-mat.str-el].